



ELSEVIER

Contents lists available at ScienceDirect

Linear Algebra and its Applications

journal homepage: www.elsevier.com/locate/laa

Extension and convergence analysis of Iterative Filtering to spherical data

Giovanni Barbarino^a, Roberto Cavassi^b, Antonio Cicone^{b,c,d,*}^a *University of Mons, Place du Parc 20, Mons, Walloon Region, B-7000, Belgium*^b *University of L'Aquila, via Vetoio n.1, L'Aquila, 67100, Italy*^c *Istituto di Astrofisica e Planetologia Spaziali, INAF, Via del Fosso del Cavaliere 100, Rome, 00133, Italy*^d *Istituto Nazionale di Geofisica e Vulcanologia, Via di Vigna Murata 605, Rome, 00143, Italy*

ARTICLE INFO

Article history:

Received 30 November 2023

Received in revised form 30 April 2024

Accepted 3 June 2024

Available online xxxxx

Submitted by V. Mehrmann

MSC:

94A12

68W40

15A18

47B06

15B05

Keywords:

Iterative Filtering

Spherical data

Convergence analysis

Nonstationary signals

Signal decomposition

ABSTRACT

Many real-life signals are defined on spherical domains, in particular in geophysics and physics applications. In this work, we tackle the problem of extending the iterative filtering algorithm, developed for the decomposition of non-stationary signals defined in Euclidean spaces, to spherical domains. We review the properties of the classical Iterative Filtering method, present its extension, and study its convergence in the discrete setting. In particular, by leveraging the Generalized Locally Toeplitz sequence theory, we are able to characterize spectrally the operators associated with the spherical extension of Iterative Filtering, and we show a counterexample of its convergence. Finally, we propose a convergent version, called Spherical Iterative Filtering, and present numerical results of its application to spherical data.

© 2024 The Author(s). Published by Elsevier Inc. This is an open access article under the CC BY license (<http://creativecommons.org/licenses/by/4.0/>).

* Corresponding author.

E-mail address: antonio.cicone@univaq.it (A. Cicone).

<https://doi.org/10.1016/j.laa.2024.06.002>

0024-3795/© 2024 The Author(s). Published by Elsevier Inc. This is an open access article under the CC BY license (<http://creativecommons.org/licenses/by/4.0/>).

1. Introduction

Real-life signals are mainly non-stationary, i.e. their features change over time or space, and are produced by nonlinear phenomena. This implies that classical signal processing methods, like Fourier or Wavelet Transform, can prove to be limited for the analysis and decomposition of such signals. For this reason in the late 90s, a group of researchers at NASA headed by Norden Huang developed a completely new approach for non-stationary signal processing called Empirical Mode Decomposition (EMD).

The EMD method, the first of its kind, is based on the iterative computation of the signal moving average via envelopes connecting its extrema. The computation of the signal moving average allows to split the signal itself into a small number of simple and non-stationary oscillatory components, called Intrinsic Mode Functions (IMFs), which are separated in frequencies and almost uncorrelated [1].

EMD proved to be a really powerful method in many applied fields of research [2–8]. However, it is prone to instability and the so-called mode-mixing [9]. For this reason, many EMD variants have been proposed over the years, like the Ensemble Empirical Mode Decomposition (EEMD) [9], the complementary EEMD [10], the complete EEMD [11], the partly EEMD [12], the noise assisted multivariate EMD (NA-MEMD) [13] and many others. They all allow us to address the instability issue as well as to reduce the so-called mode mixing problem. However, EMD and all these variants are still missing a rigorous mathematical analysis, due to the usage of a number of heuristic and ad hoc elements for the computation of the signal moving average. Some results have been presented in the literature [13–15], but a complete analysis is still missing.

Given these limitations, but also the considerable attention garnered by these methodologies within the global scientific community, numerous research groups have embarked on investigations into this domain, proffering alternative approaches to signal decomposition. Noteworthy methodologies include the Variational mode decomposition [16], sparse time-frequency representation [17,18], Blaschke decomposition [19], Geometric mode decomposition [20], Empirical wavelet transform [21], and analogous techniques [22–24]. All these techniques hinge on optimization relative to a predetermined basis.

The sole alternative method presented in existing literature founded on iterative principles and thus obviating the need for a priori assumptions about the signal under study is the Iterative Filtering (IF) algorithm [25]. We recall here also its fast implementation via FFT, denoted as Fast Iterative Filtering (FIF) [26], along with its extensions, namely Adaptive Local Iterative Filtering (ALIF) [27] and Resampled Iterative Filtering (RIF) algorithms [28,29], which are designed to handle signals characterized by pronounced non-stationarities, such as chirps, whistles, and multipath. Despite their recent publication, these iterative methods have found effective application across diverse domains [30–40].

The structural framework of the IF, ALIF, and RIF algorithms mirrors that of EMD, with the primary divergence lying in the computation of the signal moving average. Unlike EMD, these methods compute the signal moving average through convolution with

a preselected filter function, as opposed to employing the mean between two envelopes. This seemingly straightforward distinction has paved the way for a comprehensive mathematical analysis of IF, ALIF, and RIF. Notably, [26] and [14] delve into the mathematical analysis of the IF algorithm, identifying a priori conditions for its convergence. In [41], the examination of boundary effects in the IF algorithm is conducted, presenting a formula to preemptively estimate the extent of error propagation within each component of a decomposition. [42] introduces a methodology to mitigate boundary effects across decomposition algorithms, including IF, and investigates IF's efficacy in segregating components originating from stochastic processes. Building on the analyses conducted for EMD [43] and Synchrosqueezing [44], [45] scrutinizes IF's ability to disentangle two stationary frequencies within a signal. Lastly, [28], [29], and [46] delve into the convergence of the ALIF method and propose the alternative, faster, and convergent RIF algorithm.

EMD and IF methods have been extended to deal with higher dimensional [47–50] and multivariate signals [51,52] defined in a Euclidean space. Regarding the extension of this method to non-Euclidean spaces, and in particular, to the case of a sphere, a version of EMD has been proposed in the paper [53], whereas IF has never been extended yet. However, there are many interesting real-life applications in which the data are sampled on a spherical domain. We can think, for instance, of measurements regarding the Earth, like the surface temperature [54] and pressure [55], or geophysical quantities measured via satellites, like the Earth's magnetic and electric field as measured by the ESA [56], NOAA [57] and CNSA [58] missions, and the Earth's gravitational field [59], or astrophysical measurements, like the cosmic microwave background [60]. All these kinds of data have been studied so far using classical linear approaches, like spherical harmonic analysis and Fourier transform in higher dimension [61–64]. There is thus a need to develop new algorithms able to handle the nonstationarities contained in these signals.

In this work, we propose an extension of IF to spherical data and study the a priori convergence of this method in the discrete setting. The work is organized as follows: in Section 2 we review IF and introduce its generalization to the sphere. In Section 3 the theory of spectral symbol is used in order to study the convergence properties of the proposed method. The theory of Generalized Locally Toeplitz (GLT) theory is recalled in a self-contained fashion in Appendix A for the case of 2-level GLT sequences, and used to derive the results of Section 3. Section 4 reports a convergent version of Spherical Iterative Filtering (SIF) and numerical examples of its application. The paper ends with conclusions and future research directions.

2. Iterative Filtering and its adaptation to the sphere

In order to have a better understanding of how we adapted Iterative Filtering on the sphere, it is useful to have a brief description of the original algorithm.

2.1. How Iterative Filtering works

As stated in the introduction, the key difference between EMD and Iterative Filtering (IF) is the computation of the local average. As stated in the name, in IF methods the computation of the local average is made through filtering, which means convolution with a function called a filter.

Definition 1.

- (1) A function $w : [-l, l] \rightarrow \mathbb{R}$ is a filter if it is nonnegative, even, bounded, continuous, and $\int_{\mathbb{R}} w(t) dt = 1$.
- (2) A double convolution filter w is the self-convolution of a filter \tilde{w} , that is $w = \tilde{w} * \tilde{w}$.
- (3) The size, or the length, of a filter w is half the measure of its support.

Before describing the pseudo-code of Iterative Filtering, it is necessary to define the Sifting operator. This operator will be applied iteratively in the IF methods in order to extract the Intrinsic Mode Functions (IMF).

Definition 2 (Sifting operator). Let $f \in L^2(\mathbb{R})$ be a filter. The moving average of a signal $g \in \mathbb{R}^n$ can be computed as

$$\mathcal{L}(g)(x) = \int_{\mathbb{R}} g(t)f(x-t)dt. \quad (1)$$

The associated sifting operator is $\mathcal{M} : L^2(\mathbb{R}) \rightarrow L^2(\mathbb{R})$ s.t.

$$\mathcal{M}(g)(x) := (g - f * g)(x) = g(x) - \mathcal{L}(g)(x) \quad (2)$$

In practical applications we always study the signal $g(x)$ on an interval, say $[0, 1]$. Outside this interval, the signal is usually not known, so we have to impose some boundary conditions, discussed for example in [41,42]. In particular, in [42] the authors show how any signal can be pre-extended and made periodic at the boundaries, for example, by reflecting the signal on both sides and making it decay. Therefore, for simplicity and without losing generality, we will assume that the signals to be decomposed are 1-periodic.

In a discrete setting, a signal is usually given as a vector of sampled values $\mathbf{g} = [g_i]_{i=0, \dots, n-1}$ where $g_i = g(x_i)$ and $x_i = i/n$ for $i \in \mathbb{Z}$. As a consequence, one can discretize the IF moving average (1) with a simple quadrature formula

$$\mathcal{L}(g)(x_i) = \int_{\mathbb{R}} g(z)f(x_i - z) dz \approx \frac{1}{nK} \sum_{j \in \mathbb{Z}} g_j f(x_i - x_j). \quad (3)$$

Since the filter $f(z)$ has compact support of size $2L$, the above formula is always well-defined. Here K is a normalizing constant depending on $f(z)$ and n defined as

$$K := \frac{1}{n} \sum_{j \in \mathbb{Z}} f(x_i - x_j) \approx \int_{\mathbb{R}} f(z) dz = 1$$

ensuring that the quadrature formula actually performs a local convex combination of the signal points g_i , akin to the averaging operation performed by the convolution in the continuous case.

Equation (3) can be expressed through a Hermitian circulant matrix F with first row

$$\mathbf{f}_1 := \frac{1}{nLK} \left[f(0), f\left(\frac{1}{nL}\right), \dots, f\left(\frac{s}{nL}\right), 0 \dots 0, f\left(\frac{s}{nL}\right), \dots, f\left(\frac{1}{nL}\right) \right]$$

where $s = \lfloor nL \rfloor < \lfloor n/6 \rfloor$. The sampling vector of $\mathcal{M}(g)$ on the points x_0, x_1, \dots, x_{n-1} , that we indicate as $\mathcal{M}(\mathbf{g})$, is thus rewritten as a matrix-vector multiplication

$$\mathcal{M}(g)(x_i) = g_i - \mathcal{L}(g)(x_i) \implies \mathcal{M}(\mathbf{g}) = (I - F)\mathbf{g}. \tag{4}$$

Theorem 1 ([26]). *Given a signal $\mathbf{g} \in \mathbb{R}^n$, assuming that we are considering a double convolution filter, the iterated application of the Sifting operator to the sampling of the signal converges to*

$$IMF_1 = \lim_{m \rightarrow \infty} (I - F)^m \mathbf{g} = UZU^T \mathbf{g} \tag{5}$$

where Z is the diagonal binary matrix containing in the diagonal an entry equal to 1 in correspondence to each zero component of the discrete Fourier Transform of the filter f , and U is the orthogonal matrix containing, as columns, the Fourier basis vectors.

This theorem guarantees the a priori convergence of the IF algorithm for any possible signal g . The pseudocode of the discrete Iterative Filtering is reported in Algorithm 1.

Algorithm 1 Discrete Iterative Filtering $IMF = DIF(\mathbf{g})$.

```

IMF = {}
while the number of extrema of  $\mathbf{g} \geq 2$  do
  compute the filter length  $l$  for  $\mathbf{g}$  and generate the corresponding convolution matrix  $F$ 
   $\mathbf{g}_1 = \mathbf{g}$ 
  while the stopping criterion is not satisfied do
     $\mathbf{g}_{m+1} = (I - F)\mathbf{g}_m$ 
     $m = m + 1$ 
  end while
  IMF = IMF  $\cup$  { $\mathbf{g}_m$ }
   $\mathbf{g} = \mathbf{g} - \mathbf{g}_m$ 
end while
IMF = IMF  $\cup$  { $\mathbf{g}$ }

```

The algorithm would run infinitely many times. To have finite time computations it is possible to use a stopping criterion. In the literature, the standard stopping criterion used [25] is the relative error in norm 2

$$\frac{\|\mathcal{F}_m^{p+1}(\mathbf{g}_m) - \mathcal{M}_m^p(\mathbf{g}_m)\|_2}{\|\mathcal{F}_m^p(\mathbf{g}_m)\|_2} \leq \delta, \tag{6}$$

for a prefixed $\delta > 0$.

In the following, we want to extend these results to the case of the sphere.

2.2. The spherical setting

2.2.1. A useful operator

The topology of \mathbb{S}^2 is the main difference from the classic setting of Iterative Filtering. In fact, since the sphere is not diffeomorphic to a portion of \mathbb{R}^2 , at least two charts are necessary to make an atlas, as a consequence, it is impossible to extend the convolution as it is defined on \mathbb{R}^n .

In the literature, many operators have been defined on the sphere in order to adapt some of the properties of the convolution. In particular, the most interesting one that fits better our necessities is the one called isotropic convolution. Before its definition, it is necessary to describe some properties of $SO(3)$, the rotation group of the sphere.

Each point of \mathbb{S}^2 can be expressed in its spherical coordinates as $w = (\theta, \varphi)$ where $\theta \in [0, 2\pi)$ and $\varphi \in [-\pi/2, \pi/2]$. Given $f \in \mathcal{H}^0(\mathbb{S}^2)$, where $\mathcal{H}^0(\mathbb{S}^2) := \{f \in L^2(\mathbb{S}^2) : f(\theta, \varphi) = f(\theta)\}$ which is the subset of functions in $L^2(\mathbb{S}^2)$ with azimuthal/rotational symmetry about the north pole axis, it is easy to see that $\forall \rho \in SO(3), \exists r_0 \in \mathbb{S}^2$ s.t.

$$\mathcal{R}_\rho f(z) = \mathcal{R}_{r_0} f(z),$$

where $\mathcal{R}_{r_0}(f)$ can be seen as a translation of the axis of f , that now is the one passing through r_0 . That said, it is possible to introduce the following notation:

$$f_{r_0} := \mathcal{R}_{r_0} f$$

and the convention that if $f \in \mathcal{H}^0(\mathbb{S}^2)$, then $f_0 := f$.

Now we are ready to define the following.

Definition 3 (*Isotropic convolution on the sphere*). Let $g \in L^2(\mathbb{S}^2), f \in \mathcal{H}^0(\mathbb{S}^2)$, their isotropic convolution $g \circledast f$ is defined as:

$$g \circledast f(r) = \int_{\mathbb{S}^2} g(w) f_r(w) dw$$

It is useful to notice some interesting properties of this operator. First of all, the isotropic convolution is very different from a convolution, mainly for the strong requests

on the function f . Another observation is that the resulting function is defined on \mathbb{S}^2 thanks to the property mentioned above of the action of $SO(3)$ for functions in $\mathcal{H}^0(\mathbb{S}^2)$. If f was a generic function in $L^2(\mathbb{S}^2)$, the resulting function would have been defined on $SO(3)$. Finally, we present another definition of isotropic convolution that can be seen in literature [65], but it is clear that the meaning remains the same.

Definition 4 (*Isotropic convolution on the sphere*). Let $g \in L^2(\mathbb{S}^2), F \in L^2([-1, 1])$, their isotropic convolution $g \circledast F$ is defined as:

$$g \circledast F(r) = \int_{\mathbb{S}^2} g(w)F(r \cdot w)dw$$

It is easy to prove that Definition 3 and Definition 4 are equivalent when $F(n \cdot w) = f(w)$ with n being the north pole. In fact, notice that changing the vector n to r corresponds to a rotation of the function f . This alternative definition is interesting because it makes clearer the role of F as a kernel: it modulates the values of g , depending on the distance from a certain point r .

2.2.2. Adaptation of Iterative Filtering to the sphere

The isotropic convolution allows us to adapt Iterative Filtering to the spherical case. Taking f with connected support, non-negative, with $\|f\|_{L^1} = 1$ and, as requested, axially symmetric, then it can be seen as a weight function that we can use to evaluate the local average around the north pole. Hence $\int_{\mathbb{S}^2} g(w)f_r(w)dw$ can be seen as the evaluation of the local average of the function g in r , using f as a weight function on this manifold. From now on, a function f is a filter if it possesses all the above properties.

Now it is possible to define the main operator.

Definition 5 (*Sifting operator on the sphere*). Let $f \in \mathcal{H}^0(\mathbb{S}^2)$ be a filter. Its associated sifting operator is $\mathcal{M} : L^2(\mathbb{S}^2) \rightarrow L^2(\mathbb{S}^2)$ defined as

$$\mathcal{M}(g)(r) := (g - g \circledast f)(r) = g(r) - \int_{\mathbb{S}^2} g(w)f_r(w)dw$$

It is easy to show that this operator is linear and bounded. In order to have the convergence of the limit

$$\lim_{n \rightarrow \infty, n \in \mathbb{N}} \mathcal{M}^n(g) \tag{7}$$

$\forall g \in L^2(\mathbb{S}^2)$, it is necessary to prove that $\|\mathcal{M}\|_{op} \leq 1$.

Since we want to study the discretized version of this operator, we have to study if the spectral radius $\rho(\mathcal{M}) \leq 1$ for the sifting operator obtained from a certain filter function f . Since the only eigenvalue of the identity is 1, it is necessary to study the

discretized version of the operator $\cdot \otimes f$ and see when its eigenvalues are in the complex circle centered in 1 with radius 1.

To proceed, it is necessary to define the discretization grid and methods: the elements of the mesh grid are called $\{z_j\}_j$, and their associated partition of the sphere is $\{S_j\}_j$, such that $\bigcup_j S_j = \mathbb{S}^2$ and $S_i \cap S_j = \emptyset$ if $i \neq j$ and each z_j is an interior point of the associated S_j .

Now, the isotropic convolution can be written as:

$$g \otimes f(r) = \int_{\mathbb{S}^2} g(w) f_r(w) dw = \sum_j \int_{S_j} g(w) f_r(w) dw$$

If we study this operator only for g in the subspace of $L^2(\mathbb{S}^2)$ generated by $\{\chi_{S_j}\}_j$, it is possible to define the matrix associated with this operator as:

$$B_{k,j} := \frac{1}{\sigma(S_k)} \int_{S_k} \int_{S_j} f_r(w) d\sigma(w) d\sigma(r) \tag{8}$$

Where $\sigma(S_k)$ is the measure of S_k as a set on the surface of the unitary sphere. It is interesting to notice that the normalization and the first integral are necessary in order to evaluate the average of the resulting smoothed function and to project it in $\text{span}(\{\chi_{S_j}\}_j)$. On the other hand, the second integral is necessary to describe the isotropic convolution. It is easy to prove that B is stochastic since its elements are non-negative and the sum of the elements on one row is

$$\begin{aligned} \sum_j \frac{1}{\sigma(S_k)} \int_{S_k} \int_{S_j} f_r(w) d\sigma(w) d\sigma(r) &= \frac{1}{\sigma(S_k)} \int_{S_k} \int_{\mathbb{S}^2} f_r(w) d\sigma(w) d\sigma(r) \\ &= \frac{1}{\sigma(S_k)} \int_{S_k} \|f_r\|_{L^1} d\sigma(r) = 1 \end{aligned}$$

An interesting property of this class of matrix is that its spectral radius is 1.

It is useful to identify the necessary conditions for (7) to converge when the operator \mathcal{M} coincides with its discretized version $\mathbb{I} - B$.

Lemma 1. *A necessary condition for the operator limit (7) to converge when $\mathcal{M} = \mathbb{I} - B$ is that the spectrum of the associated operator B is contained in $\{z \in \mathbb{C} : \|z - 1\| \leq 1\}$.*

Proof. A necessary condition for the convergence of (7) is that the spectral radius of \mathcal{M} is ≤ 1 . Since all the eigenvalues of B are a translation of the eigenvalues of \mathcal{M} , this condition can be rewritten as $\forall \lambda \in \Lambda_B, \|1 - \lambda\| \leq 1$. In this way, we have obtained a necessary condition on the eigenvalues of B for the convergence of (7). \square

2.2.3. Conic filters and Driscoll-Healy mesh grids

Since the positivity of the eigenvalues is not granted, we choose a certain filter f_0 and study the behavior of its eigenvalues when discretized on a certain family of mesh grids on the sphere. The following function is called the truncated cone and it can be shown to be a filter.

$$f_0(\theta, \varphi) = \frac{(R - \varphi)^+}{C} = \frac{(R - d((0, 0), (\theta, \varphi)))^+}{C} \quad \text{and}$$

$$f_{(\theta', \varphi')}(\theta, \varphi) = \frac{(R - d((\theta', \varphi'), (\theta, \varphi)))^+}{C} \tag{9}$$

Where R is the radius of the filter, C a normalizing constant, and d is the spherical arc distance (called also great-circle, orthodromic or spherical distance) between two points that can be expressed as

$$d((\theta_r, \varphi_r), (\theta_w, \varphi_w)) = \arccos(\sin \varphi_r \sin \varphi_w + \cos \varphi_r \cos \varphi_w \cos(\theta_r - \theta_w)). \tag{10}$$

The grid we decided to study is similar to a Driscoll and Healy mesh grid: N^2 points equally spaced in longitude and latitude, excluding the poles. We decided to use this type of discretization since it is close to the way satellite data are collected.

We thus define the regular grid on $[0, 2\pi) \times [-\pi/2, \pi/2]$ with parameter N as

$$z_{i,j} = ((2i - 1)h, -\pi/2 + (j - 1/2)h), \quad i, j = 1, 2, \dots, N, \quad h = \frac{\pi}{N} \ll 1 \tag{11}$$

where the $z_{i,j}$ can be seen as the center of the rectangles

$$S_{i,j} = [2(i - 1)h, 2ih] \times [-\pi/2 + (j - 1)h, -\pi/2 + jh]. \tag{12}$$

Let us now consider the matrix B as defined in (8), and substitute the rectangles $S_{i,j}$ defined in (12), whose centers are the points $z_{i,j}$, to obtain

$$B_{(i,j),(p,q)} = \frac{1}{\sigma(S_{i,j})} \int_{S_{i,j}} \int_{S_{p,q}} f_r(w) d\sigma(w) d\sigma(r). \tag{13}$$

The filter in (9) is continuous and symmetric in w, r , so for $h \rightarrow 0$ one has that $f_r(w) \approx f_{z_{i,j}}(z_{p,q})$ when $r \in S_{i,j}$ and $w \in S_{p,q}$, therefore

$$B_{(i,j),(p,q)} \approx \sigma(S_{p,q}) f_{z_{i,j}}(z_{p,q}).$$

We can thus take the $N^2 \times N^2$ matrix called $B^{(N)}$ as the discretization of the isotropic convolution, whose $(i, j), (p, q)$ element is

$$B_{(i,j),(p,q)}^{(N)} = \sigma(S_{p,q}) f_{z_{i,j}}(z_{p,q}) = 2\sigma(S_{p,q}) \frac{(R - d(z_{i,j}, z_{p,q}))^+}{R - \sin(R)}, \tag{14}$$

where we substituted the value for the normalizing constant C , computed in (A.14). In the following section, we analyze the spectral properties of $B^{(N)}$ to check if it satisfies the hypotheses of Lemma 1.

Remark 1. One could approximate the moving average of the signal more precisely as

$$\int_{\mathbb{S}^2} g(w) f_r(w) d\sigma(w) \sim \sum_{p,q} g(z_{p,q}) \int_{S_{p,q}} f_r(w) d\sigma(w),$$

but it is immediate to see that

$$\left| \sigma(S_{p,q}) f_r(z_{p,q}) - \int_{S_{p,q}} f_r(w) d\sigma(w) \right| \leq \sigma(S_{p,q}) \text{diam}(S_{p,q}) = O(h^3)$$

and it is zero whenever $\text{dist}(r, S_{p,q}) \geq R$. This approximation error is so small that it can be proven to be negligible for the following analysis.

3. Spectral analysis and convergent version of the algorithm

3.1. Spectral analysis

From Lemma 1, it is evident that the spectral properties of the discretized Isotropic Convolution $B^{(N)}$ as defined in (14) are fundamental to check the convergence of the method. We thus turn to the theory of Spectral Symbols and Generalized Locally Toeplitz (GLT) sequences of matrices to analyze the asymptotic behavior of its spectrum for big N , i.e. when the mesh grid on the sphere is fine.

For the sake of the readability of the document, we postpone to Appendix A a self-contained introduction to the theory of GLT sequences, and further references for interested readers. Here we only introduce the notion of spectral symbol for a sequence of matrices that will be useful to understand the final result.

We say that a matrix-sequence $\{A^{(N)}\}_N$ admits a spectral symbol (or for short, just symbol) $f(x)$ when the sampling of $f(x)$ on a uniform n -grid over its domain yields an approximation of the eigenvalues of $A^{(N)}$, that gets better as $N \rightarrow \infty$. In a sense, the symbol encodes the asymptotic behavior of the spectrum for the whole sequence, thus proving to be an invaluable tool for the analysis of iterative methods that make use of the sequence. The same concept can be expressed also for the singular values of the matrices in the sequence, and the rigorous formal definition for the symbol is based on an ergodic formula that must hold for every test function $F \in C_c(\mathbb{C})$ ($C_c(\mathbb{R})$) as follows.

Definition 6 (*Asymptotic singular value and eigenvalue distributions of a matrix-sequence*). Let $\{A^{(N)}\}_N$ be a matrix-sequence with $A^{(N)}$ of size $N^2 \times N^2$, and let $f : \Omega \subset \mathbb{R}^d \rightarrow \mathbb{C}$ be measurable with $0 < \mu_d(\Omega) < \infty$.

- We say that $\{A^{(N)}\}_N$ has an asymptotic eigenvalue (or spectral) distribution described by f if

$$\lim_{n \rightarrow \infty} \frac{1}{N^2} \sum_{i=1}^{N^2} F(\lambda_i(A^{(N)})) = \frac{1}{\mu_d(\Omega)} \int_{\Omega} F(f(\mathbf{x})) d\mathbf{x}, \quad \forall F \in C_c(\mathbb{C}). \quad (15)$$

In this case, f is called the eigenvalue (or spectral) symbol of $\{A^{(N)}\}_N$ and we write $\{A^{(N)}\}_N \sim_{\lambda} f$.

- We say that $\{A^{(N)}\}_N$ has an asymptotic singular value distribution described by f if

$$\lim_{n \rightarrow \infty} \frac{1}{N^2} \sum_{i=1}^{N^2} F(\sigma_i(A^{(N)})) = \frac{1}{\mu_d(\Omega)} \int_{\Omega} F(|f(\mathbf{x})|) d\mathbf{x}, \quad \forall F \in C_c(\mathbb{R}). \quad (16)$$

In this case, f is called the singular value symbol of $\{A^{(N)}\}_N$ and we write $\{A^{(N)}\}_N \sim_{\sigma} f$.

We postpone to Appendix A the very technical proof of the following result, in which we identify the spectral symbol for the sequence of matrices $\{B^{(N)}\}_N$ for $N \rightarrow \infty$ as defined in (14). In this case, the symbol is referred to both the eigenvalues and the singular values of the matrices.

Theorem 2. *Let $m := RN/\pi$ and define*

$$a_{t,s}(x_1, x_2) := 6 \sin(\pi x_2) \frac{(m - \sqrt{s^2 + 4t^2 \sin(\pi x_2)^2})^+}{m^3 \pi}$$

for any $t, s \in \mathbb{Z}$. If RN is constant for any N , and $B^{(N)}$ is as in (14), then

$$\{B^{(N)}\}_N \sim_{\lambda, \sigma} \kappa(\mathbf{x}, \boldsymbol{\theta}) := \sum_{t,s \in \mathbb{Z}} a_{t,s}(\mathbf{x}) \exp(i(t\theta_1 + s\theta_2)).$$

Notice that to satisfy the hypotheses of Lemma 1, the matrix $B^{(N)}$ must in particular have all eigenvalues with nonnegative real parts. In the next section, we show that this does not always hold by studying the symbol in Theorem 2.

3.1.1. Counterexample to convergence

Already for $m = 2$ the symbol $\kappa(\mathbf{x}, \boldsymbol{\theta})$ in Theorem 4 is negative somewhere on its domain. From (A.17),

$$\kappa(\mathbf{x}, \boldsymbol{\theta}) = \sum_{t,s \in \mathbb{Z}} 3 \sin(\pi x_2) \frac{(2 - \sqrt{s^2 + 4t^2 \sin(\pi x_2)^2})^+}{4\pi} \exp(i(t\theta_1 + s\theta_2))$$

but since $m = 2$, the only nonzero terms are for $s = 1, 0, -1$, i.e.

$$\kappa(\mathbf{x}, \boldsymbol{\theta}) = \frac{3 \sin(\pi x_2)}{4\pi} \sum_{t \in \mathbb{Z}} \exp(it\theta_1) \left[2 \cos(\theta_2) (2 - \sqrt{1 + 4t^2 \sin(\pi x_2)^2})^+ + 2(1 - |t \sin(\pi x_2)|)^+ \right]$$

and for $\boldsymbol{\theta} = (0, \pi)$ we can further simplify into

$$\kappa(\mathbf{x}, (0, \pi)) = \frac{3 \sin(\pi x_2)}{2\pi} \sum_{t \in \mathbb{Z}} (1 - |t \sin(\pi x_2)|)^+ - \left(2 - \sqrt{1 + 4t^2 \sin(\pi x_2)^2} \right)^+$$

For $x_2 \rightarrow 0$, both terms in the sum become quadrature formulas that converge to definite integrals. In particular,

$$\begin{aligned} \sin(\pi x_2) \sum_{t \in \mathbb{Z}} (1 - |t \sin(\pi x_2)|)^+ &\xrightarrow{x_2 \rightarrow 0} \int_{-1}^1 1 - |x| dx = 1 \\ \sin(\pi x_2) \sum_{t \in \mathbb{Z}} \left(2 - \sqrt{1 + 4t^2 \sin(\pi x_2)^2} \right)^+ &\xrightarrow{x_2 \rightarrow 0} \int_{-1/2}^{1/2} 2 - \sqrt{1 + 4x^2} dx = 2 - \frac{\pi}{4} \end{aligned}$$

and ultimately,

$$\kappa(\mathbf{x}, (0, \pi)) \xrightarrow{x_2 \rightarrow 0} \frac{3}{2\pi} \left(\frac{\pi}{4} - 1 \right) < -0.1$$

so $\kappa(\mathbf{x}, \boldsymbol{\theta})$ is negative in an open neighborhood of the line $((x_1, 0), (0, \pi)) \in [0, 1]^2 \times [-\pi, \pi]^2$.

This example shows that whenever $R = 2\pi/N$, the symbol of the sequence $\{B^{(N)}\}_N$ is strictly negative on a non-negligible section of its domain. In turn, this means that the number of eigenvalues in $B^{(N)}$ whose real part is strictly negative will be of the order of γN^2 , where $0 < \gamma$ is constant. This is a considerable number of eigenvalues that may lead the Iterative Filtering method to fail to converge due to Lemma 1. A similar argument can be conducted for many different non-conic filters, leading to similar results.

As a consequence, we need to introduce a variation in the algorithm in order to ensure its convergence.

3.2. Convergent extension of Iterative Filtering on the sphere

From all previous results, it is clear that for generic filters, like cone filters, the extension of Iterative Filtering to spherical geometry is not convergent in general. It is possible to create a parallelism between the extension of Iterative Filtering to spherical geometry and the so-called Adaptive Local Iterative Filtering (ALIF) for 1D data. In both cases,

the filter changes size and shape point by point. In the case of spherical data, this comes as a consequence of the discretization we choose for the sphere. In ALIF this is the main feature of the algorithm. If we vectorize the data defined on the sphere that we want to decompose and treat them as if they were a 1D signal, the decomposition approach can be reformulated as a special case of the ALIF algorithm.

The convergence of ALIF, at least in the formulation presented in [27] where the scaling of the filter is done linearly point by point, is not known. But it can be made convergent by multiplying the transpose of the operator associated with the filter with the operator itself. This is what is done in the so-called SALIF algorithm [28]. The idea is that the iterative sifting operator $I - B$ applied to a discretized signal \mathbf{g} tends to extract the component of \mathbf{g} in a neighborhood of the kernel of B when the condition for convergence is satisfied. If we modify the sifting operator into $I - cB^T B$ we notice that the kernel of B is equal to the kernel of $cB^T B$ where $c > 0$ is a normalization constant chosen so that $\|cB^T B\| = 1$.

Following the same approach, in the extension of iterative filtering to spherical geometry we can substitute the operator B in (13) with the operator $cB^T B$. In doing so all eigenvalues become real, contained in the interval $[0, 1]$ and semi-simple. Hence, the algorithm converges a priori due to Lemma 2.

This is what we call from now on the Spherical Iterative Filtering (SIF) technique. The SIF pseudocode is reported in Algorithm 2.

Algorithm 2 Spherical Iterative Filtering IMF = SIF(\mathbf{g}).

```

IMF = {}
while the number of extrema of  $\mathbf{g} \geq 2$  do
  compute the filter length  $l$  for  $\mathbf{g}$  and generate the corresponding convolution matrix  $B$  and the constant
   $c = \|B\|^{-2}$ 
   $\mathbf{g}_1 = \mathbf{g}$ 
  while the stopping criterion is not satisfied do
     $\mathbf{g}_{m+1} = (I - cB^T B)\mathbf{g}_m$ 
     $m = m + 1$ 
  end while
  IMF = IMF  $\cup$   $\{\mathbf{g}_m\}$ 
   $\mathbf{g} = \mathbf{g} - \mathbf{g}_m$ 
end while
IMF = IMF  $\cup$   $\{\mathbf{g}\}$ 

```

Lemma 2. *The inner loop of Algorithm 2 always converges.*

Proof. The convergence of this algorithm has already been proved in a much more generic case in Corollary 13 of [28]. Anyway, the proof is simple.

By definition, $B^T B$ is symmetric and positive semidefinite. Moreover, thanks to the normalization constant c , all the eigenvalues of $cB^T B$ are contained in the interval $[0, 1]$. Given the eigendecomposition $cB^T B = UDU^T$ with D diagonal and U orthogonal, the inner loop of the SIF Algorithm 2 converges whenever $(I - cB^T B)^m = U(I - D)^m U^T$ converges for $m \rightarrow \infty$. As stated before, the eigenvalues of $cB^T B$ lie in $[0, 1]$, so the same holds for $(I - D)^m$ for any m , thus all their diagonal entries converge to either 0 or 1.

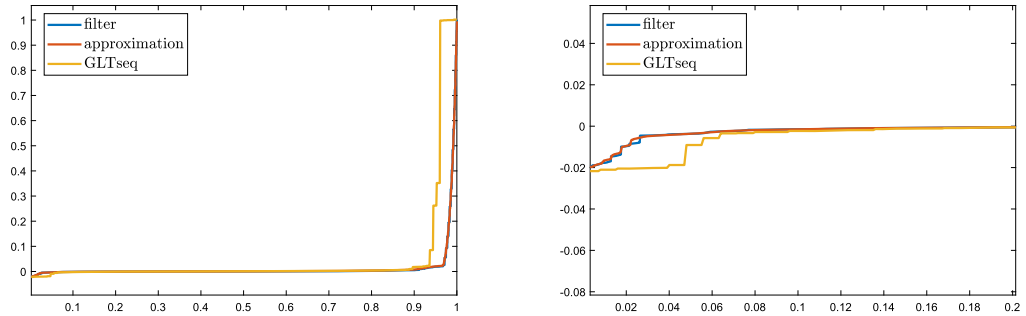


Fig. 1. In the left panel, we find the real part of the eigenvalues of B obtained using: double integration, solid blue; the approximation described in (A.18), solid red; and GLT sequence approximation, solid yellow. In the right panel, we find a zoomed-in version of the same plot on the horizontal interval $[0, 0.2]$. (For interpretation of the colors in the figure(s), the reader is referred to the web version of this article.)

Hence the algorithm converges a priori. \square

Regarding the computational complexity of Algorithm 2 it is possible to ease the computational complexity of the inner loop. A naive way to execute that part of the algorithm is to evaluate $I - cB^T B$ before the start of the while loop, then iterate a matrix-vector multiplication until the stopping criterion is satisfied. The matrix-matrix multiplication has a computational cost of $O(n^3)$, which can be simplified by not computing the full matrix $cB^T B$, but by doing a double matrix-vector multiplication $B^T(Bg_m)$ at each iteration. In doing so, the computational cost of every iteration remains $O(n^2)$, but there are no additional costs outside the loop.

Some other considerations regarding this type of algorithm can be found in [28].

4. Numerical examples

In this section, we run numerical tests of the theoretical results presented in this work.¹ In particular, in a first test, we study the spectrum of the matrix B associated with the generalization of the Iterative Filtering algorithm via straight isotropic convolution. In a second test, we apply both the direct generalization of the Iterative Filtering algorithm via isotropic convolution and the proposed convergent Spherical Iterative Filtering method to an artificial signal.

4.1. Test 1

In this first test, we evaluate the eigenvalues of the matrix B , as defined in (13), for the radius value of $\frac{\pi}{10}$ and a mesh grid as in (11) with $N = 100$.

In Fig. 1 we report the real value of the eigenvalues of B in increasing order computed using double integration, reported in solid blue, the approximation described in (A.18),

¹ Codes are available at www.cicone.com.

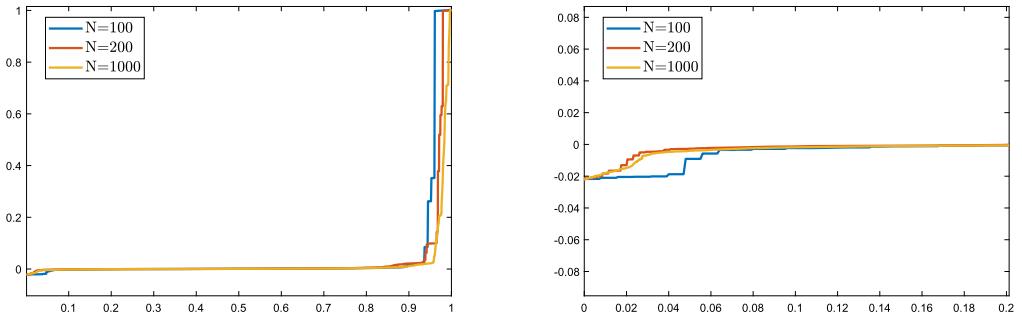


Fig. 2. In the left panel we show the real part of the eigenvalues for the GLT sequences associated with mesh grids with increasing precision. In the right panel we find a zoomed-in version of the same plot on the horizontal interval $[0, 0.2]$.

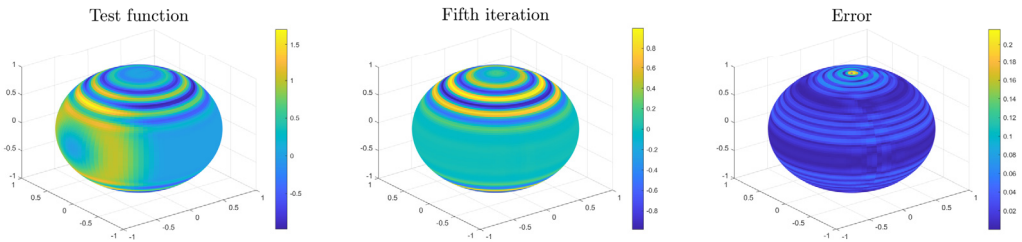


Fig. 3. Left panel: test signal containing two circular waves of different periodicity. Central panel: first component obtained applying the Sifting operator $I - B$ to the signal shown on the left panel for 5 iterations. Right panel: the error computed as the absolute value of the difference between the component obtained after 5 iterations and the ground truth component we want to extract.

solid red, and the approximation obtained using the GLT sequence. This last one, in particular, is known to represent the spectrum of the matrix up to a $o(n)$ of eigenvalues which cannot be approximated. If we zoom in on the horizontal axis on the interval $[0, 0.2]$, we can see that all approaches confirm the presence of eigenvalues with negative real parts. If we increase the grid size to $N = 200$ and $N = 1000$ we confirm the presence of eigenvalues with negative real parts, Fig. 2.

We recall that for the spectrum of $B^T B$, which is the stabilized version of the operator B which is used in the SIF algorithm, there is no need to approximate its eigenvalues since it is known a priori that they are all real and positive.

4.2. Test 2

In this second test, we apply the generalization of the Iterative Filtering algorithm via straight isotropic convolution and the SIF method, presented in Algorithm 2, to an artificial signal defined on the sphere, ref. Fig. 3 left panel. The artificial signal is constructed to contain two circular waves with different periods centered at different locations on the sphere.

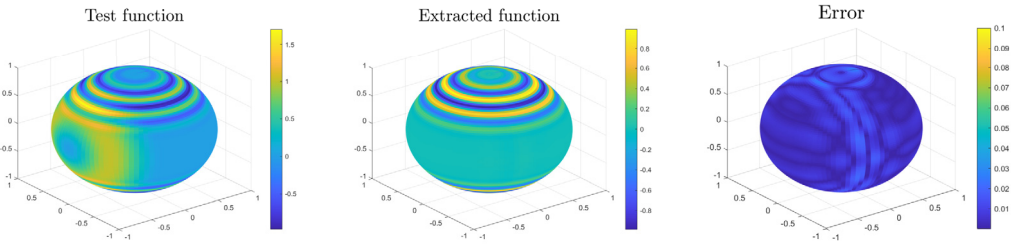


Fig. 4. Left panel: test signal containing two circular waves of different periodicity. Central panel: first component obtained applying SIF to the signal shown on the left panel for 5 iterations. Right panel: the error computed as the absolute value of the difference between the IMF obtained after 5 iterations and the ground truth component.

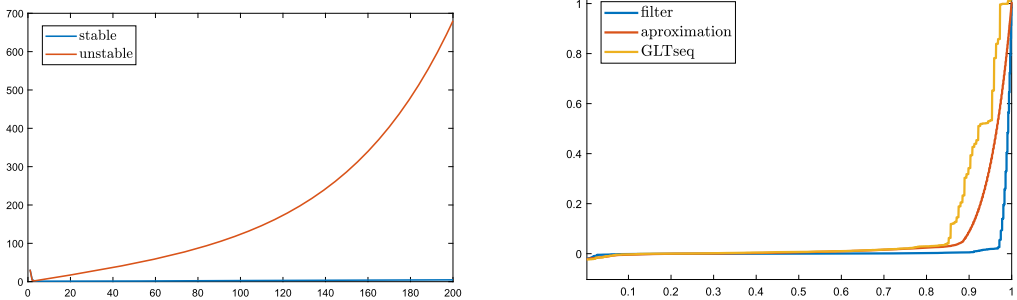


Fig. 5. Left panel: L^2 norm curves of the error for the first 200 iterations of the generalization of the Iterative Filtering algorithm via straight isotropic convolution and SIF. Right panel: a plot of the real part of the eigenvalues for the matrix B associated with a conic filter of radius $\frac{\pi}{20}$ as computed via double integration, solid blue, the approximation described in (A.18), solid red, and GLT sequence approximation, solid yellow.

We first apply the nonconvergent matrix B defined in (13) for the radius value of $\frac{\pi}{20}$ and a mesh grid as in (11) with $N = 100$. The real parts of its spectrum elements, approximated using the approaches reviewed in Test 1, are shown in the right panel in Fig. 5. Results of the application of 5 iterations of the generalization of the Iterative Filtering algorithm via straight isotropic convolution are shown in the center and right panel of Fig. 3. In particular, the central panel shows the first IMF extracted by the algorithm after 5 iterations, whereas the right panel represents the difference between this extracted IMF and the ground truth component. It is important to mention that the stopping condition (6), which is necessary in order to stop the iterative application of the Sifting operator, is not satisfied for any iteration up to 200 and the reported component in the central panel of Fig. 3 is the closest sifted signal to the ground truth reached by the algorithm in all the 200 iterations. This is another consequence of the divergence of the operator B .

In Fig. 4 we report the results obtained by applying the convergent SIF method to the same signal until the stopping criterion (6) is satisfied. In this case, the algorithm iterates 5 times. From the right panel in Fig. 4, we can see that the error is drastically reduced. It is interesting to notice that the error is stronger in the region of the sphere where the two waves meet.

If we let both algorithms run for 200 iterations and measure the L^2 norm of the error between the computed IMF and its ground truth, we obtain the curves shown in the left panel of Fig. 5. It is evident from these curves that the generalization of the Iterative Filtering algorithm via straight isotropic convolution is unstable and causes a strong energy injection, while the error associated with the SIF decomposition is bounded, having its minimum when the stopping criterion is achieved after 5 iterations. The right panel of Fig. 5 confirms the presence of eigenvalues with negative real parts in the spectrum of the matrix B used in this example.

5. Conclusions

Given the importance of developing new nonlinear algorithms for the decomposition of spherical data sets, in this work, we tackled the problem of extending the Iterative Filtering (IF) algorithm to the case of the sphere and studying its a priori convergence. After reviewing the basic properties of IF for the one-dimensional case, we introduce its extension to spherical domains in the continuous and discrete case. We leverage the theory of spectral symbols to study the convergence property of this extension of IF to the sphere. In particular, we have studied how to characterize spectrally the matrix associated with the discrete sifting operator in the spherical iterative filtering. From this analysis, we discover that the spherical iterative filtering algorithm is not guaranteed to converge, at least if we use conic filters. Following what was done in the literature for stabilizing the adaptive local iterative filtering, in this work we propose to stabilize the algorithm by multiplying the sifting operator times its transpose on the left. In doing so, the spectrum of the new operator is guaranteed to be real and contained in the interval $[0, 1]$, hence the algorithm converges a priori. We have presented numerical pieces of evidence of all these results in the numerical section. It is still an open question how to interpret from a physical point of view this new operator. We plan to tackle this problem, together with the possible acceleration of the spherical iterative filtering algorithm in future work.

Declaration of competing interest

The authors confirm that there have been no involvements that might raise the question of bias in this work or in the conclusions, implications, or opinions stated.

Data availability

Data will be made available on request.

Acknowledgement

A. Cicone, G. Barbarino, and R. Cavassi are members of the Gruppo Nazionale Calcolo Scientifico-Istituto Nazionale di Alta Matematica (GNCS-INdAM).

A. Cicone was partially supported through the GNCS-INdAM Project, CUP E53C22001930001 and CUP E53C23001670001, and thanks European Union for the financial support through “Next Generation EU” and the Italian Ministry of the University and Research for the financial support under the PRIN PNRR 2022 grant number E53D23018040001 ERC field PE1 project P2022XME5P titled “Circular Economy from the Mathematics for Signal Processing prospective”, and the Italian Ministry of the University and Research for the financial support, CUP E13C24000350001, under the “Grande Rilevanza” Italy – China Science and Technology Cooperation Joint Project titled “sCHans – Solar loading infrared thermography and deep learning techniques for the noninvasive inspection of precious artifacts”, PGR02016.

G. Barbarino acknowledges the support by the European Union, ERC consolidator grant eLinoR number 101085607, and the partial support of Alfred Kordelinin Säätiö, Grant number 210122.

R. Cavassi was partially supported through the GNCS-INdAM Project, CUP E53C23001670001, and by the PON Ph.D. project, CUP E19J21012870001.

Appendix A. GLT theory

A.1. Theory of 2-level generalized locally Toeplitz sequences

Here we recall the basic notions, results, and concepts of 2-level GLT sequences and linked subjects, without going too much into technical details. All the results we report in this section can be found more in detail in [66, Chapter 6], altogether with an extensive and complete discussion about the GLT sequences and an extension to d -level matrix sequences.

When dealing with multilevel sequences, matrices, and vectors, we will use the multi-index notation. A multi-index $\mathbf{i} \in \mathbb{N}^2$ is simply a vector in \mathbb{N}^2 ; its components are denoted by i_1, i_2 . If we write $X = [x_{\mathbf{i}\mathbf{j}}]_{\mathbf{i}, \mathbf{j}=1}^{\mathbf{n}}$, then X is a $N^2 \times N^2$ matrix whose components are indexed by two 2-indices \mathbf{i}, \mathbf{j} , both varying from $\mathbf{1} = (1, 1)$ to $\mathbf{n} = (N, N)$ according to the lexicographic ordering. In this context, by a sequence of matrices (or matrix-sequence) we mean a sequence of the form $\{A^{(N)}\}_N$ of dimension $N^2 \times N^2$. The entries of the matrix $A^{(N)}$ will be indexed by two 2-indices $\mathbf{i} = (i_1, i_2)$, $\mathbf{j} = (j_1, j_2)$, where $1 \leq i_1, i_2, j_1, j_2 \leq N$.

A.1.1. Zero-distributed sequences

A sequence of matrices $\{Z^{(N)}\}_N$ such that $\{Z^{(N)}\}_N \sim_{\sigma} 0$ is referred to as a zero-distributed sequence. In other words, $\{Z^{(N)}\}_N$ is zero-distributed iff

$$\lim_{n \rightarrow \infty} \frac{1}{N^2} \sum_{i=1}^{N^2} F(\sigma_i(Z^{(N)})) = F(0), \quad \forall F \in C_c(\mathbb{R}). \quad (\text{A.1})$$

Given a sequence of matrices $\{Z^{(N)}\}_N$, with $Z^{(N)}$ of size $N^2 \times N^2$, the following property holds. In what follows, we use the natural convention $C/\infty = 0$ for all numbers C .

Z2. $\{Z^{(N)}\}_N \sim_\sigma 0$ if there exists a $p \in [1, \infty]$ such that

$$\lim_{n \rightarrow \infty} N^{-2/p} \|Z^{(N)}\|_p = 0,$$

where $\|\cdot\|_p$ is the p -Schatten norm.

A.1.2. Approximating classes of sequences and spectral clustering

The space of matrix-sequences also presents a metric structure, induced by a distance inspired from the concept of *Approximating Class of Sequences* (a.c.s.). In fact, a sequence of matrix-sequences $\{B_m^{(N)}\}_N$ is said to be an a.c.s. for $\{A^{(N)}\}_N$ if there exist $\{E_m^{(N)}\}_N$ and $\{R_m^{(N)}\}_N$ such that for every m there exists N_m with

$$A^{(N)} = B_m^{(N)} + E_m^{(N)} + R_m^{(N)}, \quad \|E_m^{(N)}\| \leq \omega(m), \quad \text{rk}(R_m^{(N)}) \leq N^2 c(m)$$

for every $N > N_m$, and

$$\omega(m) \xrightarrow{m \rightarrow \infty} 0, \quad c(m) \xrightarrow{m \rightarrow \infty} 0.$$

In this case, we say that $\{B_m^{(N)}\}_N$ is a.c.s. convergent to $\{A^{(N)}\}_N$, and we use the notation $\{B_m^{(N)}\}_N \xrightarrow{\text{a.c.s.}} \{A^{(N)}\}_N$. In other words, $\{B_m^{(N)}\}_N$ converges to $\{A^{(N)}\}_N$ if the difference $\{A^{(N)} - B_m^{(N)}\}_N$ can be decomposed into $\{E_m^{(N)}\}_N$ of ‘small norm’ and $\{R_m^{(N)}\}_N$ of ‘small rank’.

We enunciate the main property of the a.c.s. we will need in the following.

ACS4. Let $p \in [1, \infty]$ and assume for each m there is N_m such that, for $N \geq N_m$,

$$\|A^{(N)} - B_m^{(N)}\|_p \leq \varepsilon(m, N)N^{2/p}, \quad \lim_{m \rightarrow \infty} \limsup_{N \rightarrow \infty} \varepsilon(m, N) = 0.$$

Then $\{B_m^{(N)}\}_N \xrightarrow{\text{a.c.s.}} \{A^{(N)}\}_N$.

Definition 7 (*Clustering of a sequence of matrices*). Let $\{A^{(N)}\}_N$ be a sequence of matrices, with $A^{(N)}$ of size $N^2 \times N^2$. We say that $\{A^{(N)}\}_N$ is strongly clustered at zero (in the sense of the eigenvalues), or equivalently that the eigenvalues of $\{A^{(N)}\}_N$ are strongly clustered at zero, if, for every $\varepsilon > 0$, the number of eigenvalues of $A^{(N)}$ of magnitude greater than ε is bounded by a constant C_ε independent of N ; that is, for every $\varepsilon > 0$,

$$\#\{j \in \{1, \dots, d_n\} : |\lambda_j(A_n)| > \varepsilon\} = O(1). \tag{A.2}$$

By replacing “eigenvalues” with “singular values” and $\lambda_j(A_n)$ with $\sigma_j(A_n)$ in (A.2), we obtain the definitions of a sequence of matrices strongly clustered at zero in the sense of the singular values.

A.1.3. Multilevel GLT

We now recall the theory of the multilevel generalized locally Toeplitz (GLT) sequences and symbols. A 2-level GLT sequence $\{A^{(N)}\}_N$ is a special 2-level matrix-sequence equipped with a measurable function $\kappa : [0, 1]^2 \times [-\pi, \pi]^2 \rightarrow \mathbb{C}$, the so-called GLT symbol. Unless otherwise specified, the notation

$$\{A^{(N)}\}_N \sim_{GLT} \kappa$$

means that $\{A^{(N)}\}_N$ is a 2-level GLT sequence with symbol κ . We report here the main properties of the GLT space we will make use of in this document.

GLT 1. If $\{A^{(N)}\}_N \sim_{GLT} \kappa$ then $\{A^{(N)}\}_N \sim_{\sigma} \kappa$.

GLT 2. If $\{A^{(N)}\}_N \sim_{GLT} \kappa$ and $\{A^{(N)}\}_N = \{X^{(N)}\}_N + \{Y^{(N)}\}_N$, where

- every $X^{(N)}$ is Hermitian,
- $N^{-1} \|Y^{(N)}\|_F \rightarrow 0$,

then $\{A^{(N)}\}_N \sim_{\lambda} \kappa$.

GLT 3. Here we list three important examples of GLT sequences.

- Given a function f in $L^1([-\pi, \pi]^q)$, its associated Toeplitz sequence is $\{T^{(N)}(f)\}_N$, where the elements are multidimensional Fourier coefficients of f :

$$T^{(N)}(f) = [f_{\mathbf{i}-\mathbf{j}}]_{\mathbf{i},\mathbf{j}=1}^{\mathbf{n}}, \quad f_{\mathbf{k}} = \frac{1}{(2\pi)^q} \int_{-\pi}^{\pi} f(\boldsymbol{\theta}) e^{-i\mathbf{k} \cdot \boldsymbol{\theta}} d\boldsymbol{\theta}.$$

$\{T^{(N)}(f)\}_N$ is a GLT sequence with symbol $\kappa(\mathbf{x}, \boldsymbol{\theta}) = f(\boldsymbol{\theta})$.

- Given an almost everywhere continuous function, $a : [0, 1]^q \rightarrow \mathbb{C}$, its associated diagonal sampling sequence $\{D^{(N)}(a)\}_N$ is defined as

$$D^{(N)}(a) = \text{diag} \left(\left\{ a \left(\frac{\mathbf{i}}{\mathbf{n}} \right) \right\}_{\mathbf{i}=1}^{\mathbf{n}} \right).$$

$\{D^{(N)}(a)\}_N$ is a GLT sequence with symbol $\kappa(\mathbf{x}, \boldsymbol{\theta}) = a(\mathbf{x})$.

- Any zero-distributed sequence $\{Z^{(N)}\}_N \sim_{\sigma} 0$ is a GLT sequence with symbol $\kappa(\mathbf{x}, \boldsymbol{\theta}) = 0$.

GLT 4. If $\{A^{(N)}\}_N \sim_{GLT} \kappa$ and $\{B^{(N)}\}_N \sim_{GLT} \xi$, then

- $\{(A^{(N)})^H\}_N \sim_{GLT} \bar{\kappa}$, where $(A^{(N)})^H$ is the conjugate transpose of $A^{(N)}$,
- $\{\alpha A^{(N)} + \beta B^{(N)}\}_N \sim_{GLT} \alpha\kappa + \beta\xi$ for all $\alpha, \beta \in \mathbb{C}$,
- $\{A^{(N)} B^{(N)}\}_N \sim_{GLT} \kappa\xi$.

GLT 7. $\{A^{(N)}\}_N \sim_{GLT} \kappa$ if and only if there exist GLT sequences $\{B_m^{(N)}\}_N \sim_{GLT} \kappa_m$ such that κ_m converges to κ in measure and $\{B_m^{(N)}\}_N \xrightarrow{\text{a.c.s.}} \{A^{(N)}\}_N$ as $m \rightarrow \infty$.

A.2. GLT symbol of spherical IF

A.2.1. Area and diameter of $S_{i,j}$

From classical Taylor expansion of trigonometrical functions, we get

$$\sin(a + \varepsilon) = \sin(a) + \varepsilon \cos(a) - \frac{\varepsilon^2}{2} \sin(a) - \frac{\varepsilon^3}{6} \cos(a) + \frac{\varepsilon^4}{24} \sin(a) + O(\varepsilon^5), \tag{A.3}$$

$$\cos(a + \varepsilon) = \cos(a) - \varepsilon \sin(a) - \frac{\varepsilon^2}{2} \cos(a) + O(\varepsilon^3), \tag{A.4}$$

$$\arccos(1 - \varepsilon) = \sqrt{2\varepsilon} + O(\sqrt{\varepsilon^3}), \quad \sqrt{a + \varepsilon} = \sqrt{a} + \frac{1}{2\sqrt{a}}O(\varepsilon). \tag{A.5}$$

Moreover, all the $O(\varepsilon^\alpha)$ terms above are actually bounded in absolute value by $c\varepsilon^\alpha$ where c is an absolute constant not depending on ε, α or a . From now on the same will hold true for all the $O(\cdot)$ terms in this document.

Area Recall that in polar coordinates, the differential of the normalized area measure is

$$d\sigma = \cos(\varphi)d\theta d\varphi / (4\pi). \tag{A.6}$$

Let us now compute the area and diameter on S^2 for each $S_{i,j}$.

$$\sigma(S_{i,j}) = \int \chi_{S_{i,j}}(z)d\sigma(z) = \frac{1}{4\pi} \int_{-\pi/2}^{\pi/2} \int_0^{2\pi} \chi_{S_{i,j}}(z) \cos(\varphi)d\theta d\varphi$$

and by the definition of $S_{i,j}$ in (12),

$$\begin{aligned} \sigma(S_{i,j}) &= \frac{1}{4\pi} \int_{-\pi/2+(j-1)h}^{-\pi/2+jh} \int_{2(i-1)h}^{2ih} \cos(\varphi_r)d\theta_r d\varphi_r \\ &= \frac{h}{2\pi} (\cos((j-1)h) - \cos(jh)). \end{aligned}$$

Eventually, exploiting the Taylor expansion of the cosine function (A.4),

$$\sigma(S_{i,j}) = \frac{h^2}{2\pi} \sin(jh) + O(h^3). \tag{A.7}$$

Diameter The couple of most distant points within $S_{i,j}$ is $(v_{i,j}, u_{i,j})$, the opposite corners of the rectangle, in polar coordinates,

$$v_{i,j} = (2(i-1)h, -\pi/2 + (j-1)h), \quad u_{i,j} = (2ih, -\pi/2 + jh)$$

so its diameter is the arccosine of $d_{i,j}$, where by (10),

$$d_{i,j} = \cos((j - 1)h) \cos(jh) + \sin((j - 1)h) \sin(jh) \cos(2h).$$

Expanding both sine and cosine as in (A.3) and (A.4) respectively, we get

$$\begin{aligned} d_{i,j} &= \left[\cos(jh) + h \sin(jh) - \frac{h^2}{2} \cos(jh) \right] \cos(jh) \\ &\quad + \left[\sin(jh) - h \cos(jh) - \frac{h^2}{2} \sin(jh) \right] \sin(jh) \left[1 - 2h^2 \right] + O(h^3) \\ &= 1 - \frac{h^2}{2} - 2h^2 \sin(jh)^2 + O(h^3) \end{aligned}$$

and using (A.5), we get the following formula for the diameter

$$\begin{aligned} \text{diam}(S_{i,j}) &= \arccos(d_{i,j}) = \arccos \left(1 - \frac{h^2}{2} - 2h^2 \sin(jh)^2 + O(h^3) \right) \\ &= h \sqrt{1 + 4 \sin(jh)^2} + O(h^2). \end{aligned} \tag{A.8}$$

A.2.2. Fixed diagonal

We now fix integers (t, s) with $0 \leq |t|, |s| \leq N$ to estimate the distance between $z_{i,j}$ and $z_{i-t,j-s}$ defined in (11) for $i, j, i - t, j - s$ positive integers less than N . We will only compute the first nonzero order of the distance with respect to h in the limit $N \rightarrow \infty$ or equivalently $h \rightarrow 0$. From (11), we get

$$\begin{aligned} z_{i,j} &= ((2i - 1)h, -\pi/2 + (j - 1/2)h), \\ z_{i-t,j-s} &= ((2i - 2t - 1)h, -\pi/2 + (j - s - 1/2)h) \end{aligned}$$

and it is easy to see that $d_{j,t,s}$ does not depend on i , where $d_{j,t,s} := \cos(d(z_{i,j}, z_{i-t,j-s}))$ and by (10),

$$\begin{aligned} d_{j,t,s} &= \cos((j - 1/2)h) \cos((j - s - 1/2)h) \\ &\quad + \sin((j - 1/2)h) \sin((j - s - 1/2)h) \cos(2th). \end{aligned}$$

Using classical trigonometric identities, we can rewrite it as

$$\begin{aligned} d_{j,t,s} &= \cos((j - 1/2)h) \cos((j - s - 1/2)h) + \sin((j - 1/2)h) \sin((j - s - 1/2)h) \cos(2th) \\ &= \frac{1}{2} \left[\cos(sh) + \cos((2j - s - 1)h) \right] + \frac{1}{2} \left[\cos(sh) - \cos((2j - s - 1)h) \right] \cos(2th) \\ &= \cos(sh) - \frac{1}{2} \left[\cos(sh) - \cos((2j - s - 1)h) \right] \left[1 - \cos(2th) \right]. \end{aligned} \tag{A.9}$$

Expanding the trigonometric functions following (A.3), (A.4), we see that

$$\begin{aligned}
 d_{j,t,s} &= \cos(sh) - \frac{1}{2} \left[\cos(sh) - \cos((2j - s - 1)h) \right] \left[1 - \cos(2th) \right] \\
 &= 1 - \frac{1}{2} s^2 h^2 - \frac{1}{2} \left[1 - \cos(2jh) + \sin(2jh)(s + 1)h \right] \left[2t^2 h^2 \right] \\
 &\quad + s^4 O(h^4) + t^4 O(h^4) + s^2 t^2 O(h^4) + (s + 1)^2 t^2 O(h^4) \\
 &= 1 - \frac{1}{2} h^2 \left[s^2 + 4t^2 \sin(jh)^2 + 2t^2 (s + 1) \sin(2jh)h \right] \\
 &\quad + s^2 \left[s^2 + t^2 \right] O(h^4) + t^4 O(h^4) + (s + 1)^2 t^2 O(h^4). \tag{A.10}
 \end{aligned}$$

Here we need to distinguish the cases in which $s = 0$ from the cases where $|s| > 0$.

Case $s = 0$ Consider first the case $s = 0$ and recall that $1 \leq i, j \leq N$. From (A.9),

$$d_{j,t,0} = 1 - \frac{1}{2} \left[1 - \cos((2j - 1)h) \right] \left[1 - \cos(2th) \right].$$

Notice that if we reflect with respect to the equator, i.e. we substitute j with $N + 1 - j$, the quantity does not change since

$$\cos((2j - 1)h) = \cos(2\pi + (1 - 2j)h) = \cos((2(N + 1 - j) - 1)h),$$

so from now on we suppose $j \leq N/2$ that implies, by concavity of the sin function on $[0, \pi/2]$, $\sin(jh) \geq 2jh/\pi \geq 2h/\pi$. By (A.10),

$$d_{j,t,0} = 1 - \frac{1}{2} h^2 \left[4t^2 \sin(jh)^2 + 2t^2 \sin(2jh)h \right] + t^4 O(h^4).$$

Using (A.5),

$$\begin{aligned}
 d(z_{i,j}, z_{i-t,j}) &= \arccos(d_{j,t,0}) = \arccos \left(1 - 2t^2 h^2 \sin(jh)^2 + t^2 h^3 \sin(2jh) + t^4 O(h^4) \right) \\
 &= \sqrt{4t^2 h^2 \sin(jh)^2 - 2t^2 h^3 \sin(2jh) + t^4 O(h^4)} + t^3 O(h^3) \\
 &= 2|t|h \sin(jh) + \frac{t^2 \sin(2jh) O(h^3) + t^4 O(h^4)}{4th \sin(jh)} + t^3 O(h^3) \\
 &= 2|t|h \sin(jh) + t O(h^2) + \frac{t^3 O(h^3)}{2h/\pi} + t^3 O(h^3) = 2|t|h \sin(jh) + t^3 O(h^2). \tag{A.11}
 \end{aligned}$$

If we now consider the indices $j > N/2$, we find that

$$\begin{aligned}
 d(z_{i,j}, z_{i-t,j}) &= d(z_{i,N+1-j}, z_{i-t,N+1-j}) = 2|t|h \sin((N + 1 - j)h) + t^3 O(h^2) \\
 &= 2|t|h \sin((j - 1)h) + t^3 O(h^2) = 2|t|h \sin(jh) + t^3 O(h^2)
 \end{aligned}$$

so (A.11) holds for any j . Notice moreover that if t is zero, then the above formula correctly reports that the distance is zero.

Case $s \neq 0$ Suppose now that $s \neq 0$ and in particular $|s| \geq 1$. From (A.10)

$$\begin{aligned} d_{j,t,s} &= 1 - \frac{1}{2}h^2 \left[s^2 + 4t^2 \sin(jh)^2 + 2t^2(s+1) \sin(2jh)h \right] \\ &\quad + s^2 \left[s^2 + t^2 \right] O(h^4) + t^4 O(h^4) + (s+1)^2 t^2 O(h^4) \\ &= 1 - \frac{1}{2}h^2 \left[s^2 + 4t^2 \sin(jh)^2 \right] + t^2(s+1)O(h^3) \\ &\quad + s^2 \left[s^2 + t^2 \right] O(h^4) + t^4 O(h^4) + (s+1)^2 t^2 O(h^4). \end{aligned}$$

Since $|s|, |t| \leq N$ and $h = \pi/N$, then $tO(h)$, $sO(h)$ and $(s+1)O(h)$ are all $O(1)$, so

$$t^2(s+1)O(h^3) + s^2 \left[s^2 + t^2 \right] O(h^4) + t^4 O(h^4) + (s+1)^2 t^2 O(h^4) = (|s| + |t| + 1)^3 O(h^3)$$

and thus

$$\begin{aligned} d_{j,t,s} &= \frac{h^2}{2} \left[s^2 + 4t^2 \sin(jh)^2 \right] + (|s| + |t| + 1)^3 O(h^3) \\ &= (s^2 + t^2)O(h^2) + (|s| + |t| + 1)^3 O(h^3) = (|s| + |t| + 1)^2 O(h^2). \end{aligned}$$

Using now that $s \neq 0$ we see that $[s^2 + 4t^2 \sin(jh)^2]^{-1} \leq 1/|s| \leq 1$, so

$$\begin{aligned} d(z_{i,j}, z_{i-t,j-s}) &= \arccos \left(1 - \frac{h^2}{2} \left[s^2 + 4t^2 \sin(jh)^2 \right] + (|s| + |t| + 1)^3 O(h^3) \right) \\ &= h \sqrt{[s^2 + 4t^2 \sin(jh)^2] + (|s| + |t| + 1)^3 O(h)} + (|s| + |t| + 1)^3 O(h^3) \\ &= h \sqrt{s^2 + 4t^2 \sin(jh)^2} + \frac{(|s| + |t| + 1)^3}{\sqrt{s^2 + 4t^2 \sin(jh)^2}} O(h^2) + (|s| + |t| + 1)^3 O(h^3) \\ &= h \sqrt{s^2 + 4t^2 \sin(jh)^2} + (|s| + |t| + 1)^2 O(h^2). \end{aligned} \tag{A.12}$$

Notice that we can combine (A.12) and (A.11) into one formula that holds for any s, t, j , i.e.

$$d(z_{i,j}, z_{i-t,j-s}) = h \sqrt{s^2 + 4t^2 \sin(jh)^2} + (|s| + |t| + 1)^3 O(h^2). \tag{A.13}$$

A.2.3. Normalization and support of the filter

Let the filters $f_r(w)$ be defined as

$$f_r(w) := \frac{1}{C} (R - d(r, w))^+$$

where r, w are points on \mathbb{S}^2 and $(a)^+ := \max(0, a)$. C is a constant meant to normalize the function $f_r(w)$ with respect to the measure σ . $R > 0$ is the radius of the function, and it's supposed to be less than π , so that the support of f_r is not the whole \mathbb{S}^2 .

Norm of the filter Since the norm of f_r does not depend on the point r , one can suppose that $r = (0, \pi/2)$ are its polar coordinates, so its norm will be

$$\begin{aligned} \|f_r\| = 1 &= \frac{1}{C} \int (R - d(r, w))^+ d\sigma(w) = \frac{1}{4\pi C} \int_{-\pi/2}^{\pi/2} \int_0^{2\pi} (R - d(r, w))^+ \cos(\varphi_w) d\theta_w d\varphi_w \\ &= \frac{1}{4\pi C} \int_{-\pi/2}^{\pi/2} \int_0^{2\pi} (R - \pi/2 + \varphi_w)^+ \cos(\varphi_w) d\theta_w d\varphi_w \\ &= \frac{1}{2C} \int_{\pi/2-R}^{\pi/2} (R - \pi/2 + \varphi_w) \cos(\varphi_w) d\varphi_w \\ &= \frac{1}{2C} \left[[(R - \pi/2 + \varphi_w) \sin(\varphi_w)]_{\pi/2-R}^{\pi/2} - \int_{\pi/2-R}^{\pi/2} \sin(\varphi_w) d\varphi_w \right] \\ &= \frac{1}{2C} [R - \sin(R)]. \end{aligned}$$

This proves that $C = (R - \sin(R))/2$ and thus the final expression of the filter function is

$$f_r(w) = 2 \frac{(R - d(r, w))^+}{R - \sin(R)}. \tag{A.14}$$

Support of the filter Notice that $f_r(w) \neq 0$ if and only if $d(r, w) < R$. Since $\arccos(x)$ is a strictly decreasing function on $[-1, 1]$, then it is equivalent to

$$\sin \varphi_r \sin \varphi_w + \cos \varphi_r \cos \varphi_w \cos(\theta_r - \theta_w) > \cos(R) \geq 1 - R^2/2.$$

As a consequence $f_r(w) \neq 0$ implies that

$$\begin{aligned} \frac{R^2}{2} &> 1 - \sin \varphi_r \sin \varphi_w - \cos \varphi_r \cos \varphi_w \cos(\theta_r - \theta_w) \\ &= 1 - \cos(\Delta_\varphi) + \cos \varphi_r \cos \varphi_w [1 - \cos(\Delta_\theta)] \\ &\geq \frac{1}{5} [\Delta_\varphi^2 + \cos \varphi_r \cos \varphi_w \Delta_\theta^2] \end{aligned} \tag{A.15}$$

where $\Delta_\varphi = |\varphi_r - \varphi_w|$ and $\Delta_\theta = \min\{|\theta_r - \theta_w|, 2\pi - |\theta_r - \theta_w|\}$ are both in $[0, \pi]$ and $1 - \cos(x) \geq x^2/5$ for $x \in [0, \pi]$. Suppose now that $R = mh$ with m being an absolute constant. We take $r = z_{i,j}$ and $w = z_{i-t,j-s}$ with $i, j, i - t, j - s$ integers between 1 and N , that in particular imply $|t|, |s| \leq N - 1$. Call $\tilde{j} := j - 1/2 \geq 1/2$ and assume that $f_r(w) \neq 0$. From (A.15), and (11),

$$\begin{aligned}
 5R^2 &= 5m^2h^2 > 2[\Delta_\varphi^2 + \cos \varphi_r \cos \varphi_w \Delta_\theta^2] \\
 &> 2[s^2h^2 + \sin(\tilde{j}h) \sin((\tilde{j} - s)h) \min\{2|t|h, 2\pi - 2|t|h\}^2] \\
 \implies 5m^2 &> 2[s^2 + 4 \sin(\tilde{j}h) \sin((\tilde{j} - s)h) \min\{|t|, N - |t|\}^2] \\
 \implies 3m^2 &> s^2 + 4 \sin(\tilde{j}h) \sin((\tilde{j} - s)h) \min\{|t|, N - |t|\}^2
 \end{aligned}$$

Notice that in this case $|s| < \sqrt{3}m$, i.e. $f_{z_{i,j}}(z_{i-t,j-s})$ is non-zero at most for a finite number of different values of the integer s . Since $h = \pi/N \leq \pi$,

$$\frac{\sin(x - h/2)}{\sin(x)} \geq \cos(h/2) - \sin(h/2) \tan(h)^{-1} = \frac{1}{2 \cos(h/2)} \geq \frac{1}{2} \quad \forall \pi \geq x \geq h$$

so we find that

$$3m^2 > s^2 + \sin(jh) \sin((j - s)h) \min\{|t|, N - |t|\}^2. \tag{A.16}$$

A.2.4. The discrete isotropic convolution and its symbol candidate

First, we show that the matrix sequence $\{B^{(N)}\}_N$ defined in (14) is zero-distributed as in (A.1) and all its eigenvalues are strongly clustered at zero (see (A.2)).

Lemma 3. *If the radius R of the filter does not depend on N , then the sequence $\{B^{(N)}\}_N$ is zero-distributed and shows a strong cluster at zero both for the singular values and the eigenvalues. In particular, its spectral symbol is the zero function.*

Proof. Notice that from the definition of the filter (A.14), $|f_z(w)| \leq R/C$ for any z, w , so the general element of the matrix is bounded by

$$\left| B_{(i,j),(p,q)}^{(N)} \right| \leq \frac{1}{2\pi C} Rh^2 \sin(qh) + O(h^3).$$

As a consequence, $\|B^{(N)}\|_F^2 = O(1)$ and this is sufficient to conclude that the sequence is zero distributed (by Z2) and shows a strong cluster at zero both for the singular values and the eigenvalues (See Theorems 2, 3 from [67]). Its spectral symbol can be proved to be the zero function by GLT 2. \square

To get a better understanding of the spectral properties of the matrix, we have to suppose that RN is an absolute constant for any N , meaning that R depends on N . Once this assumption is made, we can fix a 2-level diagonal (t, s) in $B^{(N)}$, and focus on the set of entries $B_{(i,j),(p,q)}^{(N)}$ for which $i - p = t$ and $j - q = s$. Our aim is to find a scalar function $a_{t,s} : [0, 1]^2 \rightarrow \mathbb{C}$ such that $a_{t,s}(ih/\pi, jh/\pi)$ converges to $B_{(i,j),(i-t,j-s)}^{(N)}$ uniformly in i, j .

Lemma 4. Suppose $R = mh$ with m constant. For any integer t, s let

$$a_{t,s}(x_1, x_2) := 6 \sin(\pi x_2) \frac{(m - \sqrt{s^2 + 4t^2 \sin(\pi x_2)^2})^+}{m^3 \pi}. \tag{A.17}$$

Then for fixed t, s

$$\max_{i,j:1 \leq i,j,i-t,j-s \leq N} \left| a_{t,s} \left(\frac{ih}{\pi}, \frac{jh}{\pi} \right) - B_{(i,j),(i-t,j-s)}^{(N)} \right| = (|t| + 1)^3 O(h) \rightarrow 0.$$

Proof. Let us thus expand each entry $B_{(i,j),(i-t,j-s)}^{(N)}$ for $h \rightarrow 0$. Substituting (A.7) into (14), we get

$$\begin{aligned} B_{(i,j),(i-t,j-s)}^{(N)} &= \sigma(S_{i-t,j-s}) f_{z_{i,j}}(z_{i-t,j-s}) \\ &= 2 \left[\frac{h^2}{2\pi} \sin((j-s)h) + O(h^3) \right] f_{z_{i,j}}(z_{i-t,j-s}). \end{aligned}$$

Recall that by (A.16), if $s \geq \sqrt{3}m$ then $f_{z_{i,j}}(z_{i-t,j-s})$, and consequentially $B_{(i,j),(i-t,j-s)}^{(N)}$, is zero and in this case

$$a_{t,s} \left(\frac{ih}{\pi}, \frac{jh}{\pi} \right) = 6 \sin(jh) \frac{(m - \sqrt{s^2 + 4t^2 \sin(jh)^2})^+}{m^3 \pi} = 0$$

so we only have to check the case $|s| < \sqrt{3}m = O(1)$. By (A.3) and (A.14) we thus find that

$$B_{(i,j),(i-t,j-s)}^{(N)} = 2 \left[\frac{h^2}{2\pi} \sin(jh) + O(h^3) \right] \frac{(R - d(z_{i,j}, z_{i-t,j-s}))^+}{R - \sin(R)}$$

and substituting $R = mh$,

$$\begin{aligned} B_{(i,j),(i-t,j-s)}^{(N)} &= 2 \left[\frac{h^2}{2\pi} \sin(jh) + O(h^3) \right] \frac{(mh - d(z_{i,j}, z_{i-t,j-s}))^+}{m^3 h^3 / 6 + O(h^5)} \\ &= 12 \left[\frac{1}{2\pi} \sin(jh) + O(h) \right] \frac{(m - d(z_{i,j}, z_{i-t,j-s})/h)^+}{m^3 + O(h^2)}. \end{aligned}$$

Here we use $1/(m^3 + O(h^2)) = 1/m^3 + O(h^2)$, and $(m - d(z_{i,j}, z_{i-t,j-s})/h)^+ \leq m = O(1)$ to see that

$$B_{(i,j),(i-t,j-s)}^{(N)} = \frac{6}{\pi} \sin(jh) \frac{(m - d(z_{i,j}, z_{i-t,j-s})/h)^+}{m^3} + O(h). \tag{A.18}$$

Substituting now the equation for the distance (A.13), and using that $g(x) := (x)^+$ is a Lipschitz function, we get

$$\begin{aligned}
 B_{(i,j),(i-t,j-s)}^{(N)} &= 6 \sin(jh) \frac{(m - \sqrt{s^2 + 4t^2 \sin(jh)^2} + (|s| + |t| + 1)^3 O(h))^+}{\pi m^3} + O(h) \\
 &= 6 \sin(jh) \frac{(m - \sqrt{s^2 + 4t^2 \sin(jh)^2})^+}{\pi m^3} + (|s| + |t| + 1)^3 O(h)
 \end{aligned}$$

where $(|s| + |t| + 1)^3 = (|t| + 1)^3 O(1)$ since we are in the case $s = O(1)$. After substituting $jh/\pi = x_2$, we eventually find the wanted function

$$a_{t,s}(x_1, x_2) := 6 \sin(\pi x_2) \frac{(m - \sqrt{s^2 + 4t^2 \sin(\pi x_2)^2})^+}{m^3 \pi}. \quad \square$$

With the functions $a_{t,s}(\mathbf{x})$ as defined in (A.17), let

$$\kappa(\mathbf{x}, \boldsymbol{\theta}) := \sum_{t,s \in \mathbb{Z}} a_{t,s}(\mathbf{x}) \exp(i(t\theta_1 + s\theta_2)) \tag{A.19}$$

where the infinite sum converges punctually everywhere for $\mathbf{x} \in [0, 1]^2$, since for every \mathbf{x} there are at most a finite number of non-zero $a_{t,s}(\mathbf{x})$, and thus a finite number of addends. In fact $a_{t,s}(\mathbf{x}) \neq 0$ implies $\sin(\pi x_2) \neq 0$, and consequently

$$m > \sqrt{s^2 + 4t^2 \sin(\pi x_2)^2} \implies \frac{m^2}{4 \sin(\pi x_2)^2} > t^2, \quad m^2 > s^2 \tag{A.20}$$

thus bounding both t and s to a finite number of integers. In the next sections, we prove that $\kappa(\mathbf{x}, \boldsymbol{\theta})$ in (A.19) is actually the GLT and spectral symbol for the matrix-sequence $\{B^{(N)}\}_N$ when RN is constant.

A.2.5. GLT symbol

Theorem 3. *If RN is constant for any N , and $B^{(N)}$ is as in (14), then*

$$\{B^{(N)}\}_N \sim_{GLT} \kappa(\mathbf{x}, \boldsymbol{\theta}) = \sum_{t,s \in \mathbb{Z}} a_{t,s}(\mathbf{x}) \exp(i(t\theta_1 + s\theta_2))$$

Proof. Call $A_M^{(N)}$ the banded matrices

$$A_M^{(N)} := \sum_{|t|,|s| \leq M} D^{(N)}(a_{t,s}(\mathbf{x})) T^{(N)}(e^{i(t\theta_1 + s\theta_2)})$$

that are GLT sequences with symbols $\{A_M^{(N)}\}_N \sim_{GLT} \kappa_M(\mathbf{x}, \boldsymbol{\theta}) := \sum_{|t|,|s| \leq M} a_{t,s}(\mathbf{x}) \times e^{i(t\theta_1 + s\theta_2)}$ due to **GLT 3** and **GLT 4**. In (A.20) we have already proved that $\kappa_M(\mathbf{x}, \boldsymbol{\theta})$ converge everywhere to $\kappa(\mathbf{x}, \boldsymbol{\theta})$, so we only need to show that $\{A_M^{(N)}\}_N \xrightarrow{a.c.s.} \{B^{(N)}\}_N$ since by **GLT 7** it would automatically prove the thesis.

Recall that by (A.17)

$$a_{t,s}(x_1, x_2) = 6 \sin(\pi x_2) \frac{(m - \sqrt{s^2 + 4t^2 \sin(\pi x_2)^2})^+}{m^3 \pi}$$

and by Lemma 4, (A.16) and (A.18),

$$B_{(i,j),(i-t,j-s)}^{(N)} = 6 \sin(jh) \frac{(m - \sqrt{s^2 + 4t^2 \sin(jh)^2})^+}{\pi m^3} + (|t| + 1)^3 O(h) \tag{A.21}$$

$$= 6 \sin(jh) \frac{(m - d(z_{i,j}, z_{i-t,j-s})/h)^+}{\pi m^3} + O(h) \tag{A.22}$$

holds for any i, j, t, s such that $1 \leq i, i - t, j, j - s \leq N$, $|t| < N$, $|s| < \sqrt{3}m$, otherwise it is zero. Suppose from now on that $\max\{1, \sqrt{3}m\} < M \leq N$, so that we can write down the entries of $A_M^{(N)}$ as

$$[A_M^{(N)}]_{(i,j),(i-t,j-s)} = \begin{cases} a_{t,s}(ih/\pi, jh/\pi) = 6 \sin(jh) \frac{(m - \sqrt{s^2 + 4t^2 \sin(jh)^2})^+}{m^3 \pi}, & |s|, |t| \leq M, \\ 0, & \text{otherwise.} \end{cases} \tag{A.23}$$

We now estimate the difference between $A_M^{(N)}$ and $B^{(N)}$ as

$$\begin{aligned} \|B^{(N)} - A_M^{(N)}\|_F^2 &= \sum_{|t|, |s| \leq M} \sum_{\substack{i,j: \\ 1 \leq i, i-t, j, j-s \leq N}} \left| B_{(i,j),(i-t,j-s)}^{(N)} - [A_M^{(N)}]_{(i,j),(i-t,j-s)} \right|^2 \\ &+ \sum_{N > |t| > M} \sum_{|s| \leq \sqrt{3}m} \sum_{\substack{i,j: \\ 1 \leq i, i-t, j, j-s \leq N}} \left| B_{(i,j),(i-t,j-s)}^{(N)} \right|^2 \end{aligned}$$

where the second multi-sum has no elements with $|s| > M > \sqrt{3}m$ because that would lead to $B_{(i,j),(i-t,j-s)}^{(N)} = 0$. The first term is easy to bound thanks to (A.21) and (A.23).

$$\begin{aligned} &\sum_{|t|, |s| \leq M} \sum_{\substack{i,j: \\ 1 \leq i, i-t, j, j-s \leq N}} \left| B_{(i,j),(i-t,j-s)}^{(N)} - [A_M^{(N)}]_{(i,j),(i-t,j-s)} \right|^2 \\ &= \sum_{|t|, |s| \leq M} \sum_{\substack{i,j: \\ 1 \leq i, i-t, j, j-s \leq N}} (|t| + 1)^6 O(h^2) = O(1). \end{aligned}$$

For the second term, we notice that the expression in (A.22) does not depend on i , since $d(z_{i,j}, z_{i-t,j-s}) = d_{j,t,s}$ as in (A.9), and that for a fixed t , there are at most $n - |t|$ indices i such that $1 \leq i, i - t \leq N$, so

$$\sum_{N > |t| > M} \sum_{|s| \leq M} \sum_{\substack{i,j: \\ 1 \leq i, i-t, j, j-s \leq N}} \left| B_{(i,j),(i-t,j-s)}^{(N)} \right|^2$$

$$\begin{aligned}
 &= \sum_{N>|t|>M} \sum_{|s|\leq M} \sum_{\substack{i,j: \\ 1\leq i,i-t,j,j-s\leq N}} \frac{36 \sin(jh)^2}{\pi^2 m^6} [(m - d(z_{i,j}, z_{i-t,j-s})/h)^+]^2 + O(h) \\
 &\leq \sum_{N>|t|>M} \sum_{|s|\leq M} \sum_{\substack{j: \\ 1\leq j,j-s\leq N}} (N - |t|) \frac{36 \sin(jh)^2}{\pi^2 m^4} + O(1) \\
 &= \sum_{N>|t|>M} \sum_{1\leq j\leq N} (N - |t|) \frac{36(2M + 1) \sin(jh)^2}{\pi^2 m^4} + O(1)
 \end{aligned}$$

Now we split the sum in j depending on whether $\min\{j, N - j\} \leq 2\sqrt{3}m$ or not. If it holds, then

$$\sin(jh) = \sin((N - j)h) \leq 2\sqrt{3}mh = O(h)$$

and

$$\begin{aligned}
 &\sum_{N>|t|>M} \sum_{j:\min\{j,N-j\}\leq 2\sqrt{3}m} (N - |t|) \frac{36(2M + 1) \sin(jh)^2}{\pi^2 m^4} + O(1) \\
 &= \sum_{N>|t|>M} \sum_{j:\min\{j,N-j\}\leq 2\sqrt{3}m} O(1) = O(N)
 \end{aligned}$$

Otherwise, we have $2\sqrt{3}m < j < N - 2\sqrt{3}m$ and in particular, $N > 4\sqrt{3}m$. Keeping in mind that $|s| \leq \sqrt{3}m$, then

$$\begin{aligned}
 \frac{\sin((j - s)h)}{\sin(jh)} &= \cos(sh) - \sin(sh) \tan(jh)^{-1} \\
 &\geq \begin{cases} \cos(sh) - \sin(sh) \tan(2\sqrt{3}mh)^{-1} & s \geq 0 \\ \cos(sh) - \sin(sh) \tan(-2\sqrt{3}mh)^{-1} & s < 0 \end{cases} \\
 &= \frac{\sin((2\sqrt{3}m - |s|)h)}{\sin(2\sqrt{3}mh)} \geq \frac{\sin(\sqrt{3}mh)}{\sin(2\sqrt{3}mh)} = \frac{1}{2 \cos(\sqrt{3}mh)} \geq \frac{1}{2}.
 \end{aligned}$$

By the relation (A.16), the entry $B_{(i,j),(i-t,j-s)}^{(N)}$ is zero when

$$\min\{|t|, N - |t|\}^2 \sin(jh) \sin((j - s)h) \geq \min\{|t|, N - |t|\}^2 \sin(jh)^2 / 2 \geq 3m^2 \geq 3m^2 - s^2 \tag{A.24}$$

so we can restrict the index t to $\min\{|t|, N - |t|\} < \sqrt{6}m / \sin(jh)$ in the sum and find that

$$\sum_{N>|t|>M} \sum_{2\sqrt{3}m < j < N - 2\sqrt{3}m} (N - |t|) \frac{36(2M + 1) \sin(jh)^2}{\pi^2 m^4} + O(1)$$

$$\begin{aligned}
 &= \sum_{2\sqrt{3}m < j < N - 2\sqrt{3}m} \sum_{\substack{N > |t| > M \\ \min\{|t|, N - |t|\} < \sqrt{6}m / \sin(jh)}} (N - |t|) \sin(jh)^2 O(1) + O(1) \\
 &\leq \sum_{2\sqrt{3}m < j < N - 2\sqrt{3}m} 2 \left[N \left(\frac{\sqrt{6}m}{\sin(jh)} - M + 1 \right)^+ + \frac{6m^2}{\sin(jh)^2} \right] \sin(jh)^2 O(1) + \frac{1}{\sin(jh)} O(1) \\
 &\leq \sum_{1 \leq j < N} \left(\sqrt{6}m - (M - 1) \sin(jh) \right)^+ \sin(jh) O(N) + O(1) + \frac{1}{\sin(jh)} O(1).
 \end{aligned}$$

Since $\sin(jh) = \sin((N - j)h)$, we can bound the sum by doubling it and stop the index at $j = \lfloor N/2 \rfloor$. Under this hypothesis we have the bounds $jh \geq \sin(jh) \geq 2jh/\pi$ leading to $\sum_{j=1}^{\lfloor N/2 \rfloor} 1/\sin(jh) \leq \sum_{j=1}^{\lfloor N/2 \rfloor} \pi/(2jh) = O(N \log(N))$ and

$$\begin{aligned}
 &\sum_{N > |t| > M} \sum_{2\sqrt{3}m < j < N - 2\sqrt{3}m} (N - |t|) \frac{36(2M + 1) \sin(jh)^2}{\pi^2 m^4} + O(1) \\
 &\leq \left[\sum_{1 \leq j \leq \lfloor N/2 \rfloor} \left(\sqrt{6}m - \frac{2(M - 1)h}{\pi} j \right)^+ j O(1) \right] + O(N \log(N)). \\
 &\leq \left[\sum_{1 \leq j < \frac{\sqrt{6}\pi m}{2(M - 1)h}} \sqrt{6}m \cdot j O(1) \right] + O(N \log(N)) \\
 &\leq \frac{6\pi^2 m^2}{4(M - 1)^2 h^2} O(1) + O(N \log(N)) = \frac{1}{(M - 1)^2} O(N^2) + O(N \log(N)).
 \end{aligned}$$

Putting all the terms together, we find that

$$\begin{aligned}
 \|B^{(N)} - A_M^{(N)}\|_F^2 &= O(1) + O(N) + \frac{1}{(M - 1)^2} O(N^2) + O(N \log(N)) \\
 &= \left[\frac{1}{(M - 1)^2} O(1) + O\left(\frac{\log(N)}{N}\right) \right] \cdot N^2
 \end{aligned}$$

and we conclude thanks to ACS 4 with $p = 2$ and

$$\lim_{M \rightarrow \infty} \limsup_{N \rightarrow \infty} \varepsilon(M, N) = \lim_{M \rightarrow \infty} \limsup_{N \rightarrow \infty} \sqrt{\frac{1}{(M - 1)^2} O(1) + O\left(\frac{\log(N)}{N}\right)} = 0. \quad \square$$

Notice that in particular this shows that in the hypotheses of Theorem 3, $\{B^{(N)}\}_N \sim_{\sigma} \kappa(\mathbf{x}, \boldsymbol{\theta})$ by GLT 1.

A.2.6. Spectral symbol

Here we show that $\{B^{(N)}\}_N$ has spectral symbol $\kappa(\mathbf{x}, \boldsymbol{\theta})$. To do so, we need to prove that it is close enough to a Hermitian matrix in Frobenius norm, i.e. its skew-Hermitian part is small, and conclude thanks to **GLT 2**.

Theorem 4. *If R_N is constant for any N , and $B^{(N)}$ is as in (14), then*

$$\{B^{(N)}\}_N \sim_{\lambda} \kappa(\mathbf{x}, \boldsymbol{\theta}) = \sum_{t,s \in \mathbb{Z}} a_{t,s}(\mathbf{x}) \exp(i(t\theta_1 + s\theta_2))$$

Proof. Let $E^{(N)}$ be 2 times the skew-Hermitian part of $B^{(N)}$, i.e. $E^{(N)} := B^{(N)} - [B^{(N)}]^H$. By (A.16), if $|s| \geq \sqrt{3}m$ then the elements $B_{(i,j),(i-t,j-s)}^{(N)}$ and $[B^{(N)}]_{(i,j),(i-t,j-s)}^H = B_{(i-t,j-s),(i,j)}^{(N)}$ are both zero, so $E_{(i,j),(i-t,j-s)}^{(N)}$ is zero too and thus we can focus on the case $s < \sqrt{3}m = O(1)$. By definition (14), equation (A.18) and using that the distance $d(r, w)$ is symmetric in r, w , we have

$$E_{(i,j),(i-t,j-s)}^{(N)} = 6[\sin(jh) - \sin((j-s)h)] \frac{(m - d(z_{i,j}, z_{i-t,j-s})/h)^+}{\pi m^3} + O(h)$$

but since $|s| < \sqrt{3}m$,

$$\begin{aligned} |\sin(jh) - \sin((j-s)h)| &= |\sin(jh)[1 - \cos(sh)] + \cos(jh)\sin(sh)| \\ &\leq |1 - \cos(sh)| + |\sin(sh)| \leq \frac{s^2 h^2}{2} + sh \end{aligned}$$

and thus $E_{(i,j),(i-t,j-s)}^{(N)} = O(h)$. As a consequence, its Frobenius norm is bounded by

$$\|E^{(N)}\|_F^2 = \sum_{|s| < \sqrt{3}m} \sum_{|t| < N} \sum_{\substack{i,j: \\ 1 \leq i, i-t, j, j-s \leq N}} \left| E_{(i,j),(i-t,j-s)}^{(N)} \right|^2 = N^3 O(h^2) = O(N) = o(N^2).$$

If $\tilde{B}^{(N)} := (B^{(N)} + [B^{(N)}]^H)/2$ is the Hermitian part of $B^{(N)}$, then

$$\|B^{(N)} - \tilde{B}^{(N)}\|_F^2 = \frac{1}{4} \|E^{(N)}\|_F^2 = o(N^2)$$

and since $\{B^{(N)}\}_N \sim_{GLT} \kappa(\mathbf{x}, \boldsymbol{\theta})$ by Theorem 3, then $\kappa(\mathbf{x}, \boldsymbol{\theta})$ is also the spectral symbol of $\{B^{(N)}\}_N$ thanks to **GLT 2**. \square

References

[1] N.E. Huang, Z. Shen, S.R. Long, M.C. Wu, H.H. Shih, Q. Zheng, N.-C. Yen, C.C. Tung, H.H. Liu, The empirical mode decomposition and the Hilbert spectrum for nonlinear and non-stationary time series analysis, *Proc. R. Soc., Math. Phys. Eng. Sci.* 454 (1971) (1998) 903–995.

- [2] H. Abbasimehr, M. Shabani, M. Yousefi, An optimized model using lstm network for demand forecasting, *Comput. Ind. Eng.* 143 (2020) 106435.
- [3] J. Cao, Z. Li, J. Li, Financial time series forecasting model based on ceemdan and lstm, *Physica A* 519 (2019) 127–139.
- [4] H. Cui, Y. Guan, H. Chen, Rolling element fault diagnosis based on vmd and sensitivity mckd, *IEEE Access* 9 (2021) 120297–120308.
- [5] K. Holmberg, A. Erdemir, Influence of tribology on global energy consumption, costs and emissions, *Friction* 5 (2017) 263–284.
- [6] A. Stetco, F. Dinmohammadi, X. Zhao, V. Robu, D. Flynn, M. Barnes, J. Keane, G. Nenadic, Machine learning methods for wind turbine condition monitoring: a review, *Renew. Energy* 133 (2019) 620–635.
- [7] L. Zeng, B.D. Wardlow, D. Xiang, S. Hu, D. Li, A review of vegetation phenological metrics extraction using time-series, multispectral satellite data, *Remote Sens. Environ.* 237 (2020) 111511.
- [8] P. Zhang, J.-H. Jeong, J.-H. Yoon, H. Kim, S.-Y.S. Wang, H.W. Linderholm, K. Fang, X. Wu, D. Chen, Abrupt shift to hotter and drier climate over inner East Asia beyond the tipping point, *Science* 370 (6520) (2020) 1095–1099.
- [9] Z. Wu, N.E. Huang, Ensemble empirical mode decomposition: a noise-assisted data analysis method, *Adv. Adapt. Data Anal.* 1 (01) (2009) 1–41.
- [10] J.-R. Yeh, J.-S. Shieh, N.E. Huang, Complementary ensemble empirical mode decomposition: a novel noise enhanced data analysis method, *Adv. Adapt. Data Anal.* 2 (02) (2010) 135–156.
- [11] M.E. Torres, M.A. Colominas, G. Schlotthauer, P. Flandrin, A complete ensemble empirical mode decomposition with adaptive noise, in: 2011 IEEE International Conference on Acoustics, Speech and Signal Processing (ICASSP), IEEE, 2011, pp. 4144–4147.
- [12] J. Zheng, J. Cheng, Y. Yang, Partly ensemble empirical mode decomposition: an improved noise-assisted method for eliminating mode mixing, *Signal Process.* 96 (2014) 362–374.
- [13] N. Ur Rehman, D.P. Mandic, Filter bank property of multivariate empirical mode decomposition, *IEEE Trans. Signal Process.* 59 (5) (2011) 2421–2426.
- [14] C. Huang, L. Yang, Y. Wang, Convergence of a convolution-filtering-based algorithm for empirical mode decomposition, *Adv. Adapt. Data Anal.* 1 (04) (2009) 561–571.
- [15] N.E. Huang, Introduction to the Hilbert–Huang transform and its related mathematical problems, in: *Hilbert–Huang Transform and Its Applications*, World Scientific, 2014, pp. 1–26.
- [16] K. Dragomiretskiy, D. Zosso, Variational mode decomposition, *IEEE Trans. Signal Process.* 62 (3) (2013) 531–544.
- [17] T.Y. Hou, Z. Shi, Adaptive data analysis via sparse time-frequency representation, *Adv. Adapt. Data Anal.* 3 (01n02) (2011) 1–28.
- [18] T.Y. Hou, M.P. Yan, Z. Wu, A variant of the emd method for multi-scale data, *Adv. Adapt. Data Anal.* 1 (04) (2009) 483–516.
- [19] R.R. Coifman, S. Steinerberger, H.-t. Wu, Carrier frequencies, holomorphy, and unwinding, *SIAM J. Math. Anal.* 49 (6) (2017) 4838–4864.
- [20] S. Yu, J. Ma, S. Osher, Geometric mode decomposition, *Inverse Probl. Imaging* 12 (4) (2018).
- [21] J. Gilles, Empirical wavelet transform, *IEEE Trans. Signal Process.* 61 (16) (2013) 3999–4010.
- [22] S. Meignen, V. Perrier, A new formulation for empirical mode decomposition based on constrained optimization, *IEEE Signal Process. Lett.* 14 (12) (2007) 932–935.
- [23] N. Pustelnik, P. Borgnat, P. Flandrin, A multicomponent proximal algorithm for empirical mode decomposition, in: 2012 Proceedings of the 20th European Signal Processing Conference (EUSIPCO), IEEE, 2012, pp. 1880–1884.
- [24] I.W. Selesnick, Resonance-based signal decomposition: a new sparsity-enabled signal analysis method, *Signal Process.* 91 (12) (2011) 2793–2809.
- [25] L. Lin, Y. Wang, H. Zhou, Iterative filtering as an alternative algorithm for empirical mode decomposition, *Adv. Adapt. Data Anal.* 1 (04) (2009) 543–560.
- [26] A. Cicone, H. Zhou, Numerical analysis for iterative filtering with new efficient implementations based on fft, *Numer. Math.* 147 (1) (2021) 1–28.
- [27] A. Cicone, J. Liu, H. Zhou, Adaptive local iterative filtering for signal decomposition and instantaneous frequency analysis, *Appl. Comput. Harmon. Anal.* 41 (2) (2016) 384–411.
- [28] G. Barbarino, A. Cicone, Stabilization and variations to the adaptive local iterative filtering algorithm: the fast resampled iterative filtering method, *Numer. Math.* 156 (2024) 395–433.
- [29] G. Barbarino, A. Cicone, Conjectures on spectral properties of alif algorithm, *Linear Algebra Appl.* 647 (2022) 127–152.

- [30] H. Ghobadi, L. Spogli, L. Alfonsi, C. Cesaroni, A. Cicone, N. Linty, V. Romano, M. Cafaro, Disentangling ionospheric refraction and diffraction effects in gnss raw phase through fast iterative filtering technique, *GPS Solut.* 24 (3) (2020) 85.
- [31] Y. Li, X. Wang, Z. Liu, X. Liang, S. Si, The entropy algorithm and its variants in the fault diagnosis of rotating machinery: a review, *IEEE Access* 6 (2018) 66723–66741.
- [32] M. Materassi, M. Piersanti, G. Consolini, P. Diego, G. D'Angelo, I. Bertello, A. Cicone, Stepping into the equatorward boundary of the auroral oval: preliminary results of multi scale statistical analysis, *Ann. Geophys.* 62 (4) (2019) GM455.
- [33] I. Mitiche, G. Morison, A. Nesbitt, M. Hughes-Narborough, B.G. Stewart, P. Boreham, Classification of partial discharge signals by combining adaptive local iterative filtering and entropy features, *Sensors* 18 (2) (2018) 406.
- [34] E. Papini, A. Cicone, M. Piersanti, L. Franci, P. Hellinger, S. Landi, A. Verdini, Multidimensional iterative filtering: a new approach for investigating plasma turbulence in numerical simulations, *J. Plasma Phys.* 86 (5) (2020) 871860501.
- [35] G. Piersanti, M. Piersanti, A. Cicone, P. Canofari, M. Di Domizio, An inquiry into the structure and dynamics of crude oil price using the fast iterative filtering algorithm, *Energy Econ.* 92 (2020) 104952.
- [36] M. Piersanti, M. Materassi, R. Battiston, V. Carbone, A. Cicone, G. D'Angelo, P. Diego, P. Ubertini, Magnetospheric–ionospheric–lithospheric coupling model. 1: observations during the 5 August 2018 Bayan earthquake, *Remote Sens.* 12 (20) (2020) 3299.
- [37] R. Sharma, R.B. Pachori, A. Upadhyay, Automatic sleep stages classification based on iterative filtering of electroencephalogram signals, *Neural Comput. Appl.* 28 (2017) 2959–2978.
- [38] L. Spogli, M. Piersanti, C. Cesaroni, M. Materassi, A. Cicone, L. Alfonsi, V. Romano, R.G. Ezquer, Role of the external drivers in the occurrence of low-latitude ionospheric scintillation revealed by multi-scale analysis, *J. Space Weather Space Clim.* 9 (2019) A35.
- [39] L. Spogli, H. Ghobadi, A. Cicone, L. Alfonsi, C. Cesaroni, N. Linty, V. Romano, M. Cafaro, Adaptive phase detrending for gnss scintillation detection: a case study over Antarctica, *IEEE Geosci. Remote Sens. Lett.* 19 (2021) 1–5.
- [40] Z.-G. Yu, V. Anh, Y. Wang, D. Mao, J. Wanliss, Modeling and simulation of the horizontal component of the geomagnetic field by fractional stochastic differential equations in conjunction with empirical mode decomposition, *J. Geophys. Res. Space Phys.* 115 (A10) (2010).
- [41] A. Cicone, P. Dell'Acqua, Study of boundary conditions in the iterative filtering method for the decomposition of nonstationary signals, *J. Comput. Appl. Math.* 373 (2020) 112248.
- [42] A. Stallone, A. Cicone, M. Materassi, New insights and best practices for the successful use of empirical mode decomposition, iterative filtering and derived algorithms, *Sci. Rep.* 10 (1) (2020) 15161.
- [43] G. Rilling, P. Flandrin, One or two frequencies? The empirical mode decomposition answers, *IEEE Trans. Signal Process.* 56 (1) (2007) 85–95.
- [44] H.-T. Wu, P. Flandrin, I. Daubechies, One or two frequencies? The synchrosqueezing answers, *Adv. Adapt. Data Anal.* 3 (01–02) (2011) 29–39.
- [45] A. Cicone, S. Serra-Capizzano, H. Zhou, One or two frequencies? The iterative filtering answers, *Appl. Math. Comput.* 462 (2024) 128322.
- [46] A. Cicone, C. Garoni, S. Serra-Capizzano, Spectral and convergence analysis of the discrete alif method, *Linear Algebra Appl.* 580 (2019) 62–95.
- [47] A. Cicone, H. Zhou, Multidimensional iterative filtering method for the decomposition of high-dimensional non-stationary signals, *Numer. Math.* 10 (2) (2017) 278–298.
- [48] G. Rilling, P. Flandrin, P. Gonçalves, J.M. Lilly, Bivariate empirical mode decomposition, *IEEE Signal Process. Lett.* 14 (12) (2007) 936–939.
- [49] T. Tanaka, D.P. Mandic, Complex empirical mode decomposition, *IEEE Signal Process. Lett.* 14 (2) (2007) 101–104.
- [50] M.R. Thirumalaisamy, P.J. Ansell, Fast and adaptive empirical mode decomposition for multidimensional, multivariate signals, *IEEE Signal Process. Lett.* 25 (10) (2018) 1550–1554.
- [51] A. Cicone, E. Pellegrino, Multivariate fast iterative filtering for the decomposition of nonstationary signals, *IEEE Trans. Signal Process.* 70 (2022) 1521–1531.
- [52] N. Rehman, D.P. Mandic, Multivariate empirical mode decomposition, *Proc. R. Soc. A, Math. Phys. Eng. Sci.* 466 (2117) (2010) 1291–1302.
- [53] N. Fauchereau, G. Pegram, S. Sinclair, Empirical mode decomposition on the sphere: application to the spatial scales of surface temperature variations, *Hydrol. Earth Syst. Sci.* 12 (3) (2008) 933–941.

- [54] X. Yun, B. Huang, J. Cheng, W. Xu, S. Qiao, Q. Li, A new merge of global surface temperature datasets since the start of the 20th century, *Earth Syst. Sci. Data* 11 (4) (2019) 1629–1643.
- [55] A. Sweeney, G. Mungov, L. Wright, Products and services available from us noaa ncei archive of water level data, in: EGU General Assembly Conference Abstracts, 2021, pp. EGU21–8027.
- [56] E. Friis-Christensen, H. Lühr, G. Hulot, Swarm: a constellation to study the Earth's magnetic field, *Earth Planets Space* 58 (2006) 351–358.
- [57] T. Loto'aniu, R. Redmon, S. Califf, H. Singer, W. Rowland, S. Macintyre, C. Chastain, R. Dence, R. Bailey, E. Shoemaker, et al., The goes-16 spacecraft science magnetometer, *Space Sci. Rev.* 215 (2019) 1–28.
- [58] J. Cao, L. Zeng, F. Zhan, Z. Wang, Y. Wang, Y. Chen, Q. Meng, Z. Ji, P. Wang, Z. Liu, et al., The electromagnetic wave experiment for cses mission: search coil magnetometer, *Sci. China, Technol. Sci.* 61 (2018) 653–658.
- [59] J. Marsh, F. Lerch, B. Putney, D. Christodoulidis, D. Smith, T. Felsentreger, B. Sanchez, S. Klosko, E. Pavlis, T. Martin, et al., A new gravitational model for the Earth from satellite tracking data: gem-t1, *J. Geophys. Res., Solid Earth* 93 (B6) (1988) 6169–6215.
- [60] M. Kamionkowski, A. Kosowsky, The cosmic microwave background and particle physics, *Annu. Rev. Nucl. Part. Sci.* 49 (1) (1999) 77–123.
- [61] W. Hu, S. Dodelson, Cosmic microwave background anisotropies, *Annu. Rev. Astron. Astrophys.* 40 (1) (2002) 171–216.
- [62] S. Klosko, C. Wagner, Spherical harmonic representation of the gravity field from dynamic satellite data, *Planet. Space Sci.* 30 (1) (1982) 5–28.
- [63] J. Pierret, Optimal global average annual mean temperature estimation using station data and spherical harmonics, Ph.D. thesis, San Diego State University, 2013.
- [64] E. Thébault, G. Hulot, B. Langlais, P. Vigneron, A spherical harmonic model of Earth's lithospheric magnetic field up to degree 1050, *Geophys. Res. Lett.* 48 (21) (2021) e2021GL095147.
- [65] R.A. Kennedy, T.A. Lamahewa, L. Wei, On azimuthally symmetric 2-sphere convolution, *Digit. Signal Process.* 21 (5) (2011) 660–666, dASP 2009 - Defense applications of signal processing.
- [66] C. Geroni, S. Serra-Capizzano, Generalized Locally Toeplitz Sequences: Theory and Applications, vol. 2, 2018, pp. 1–194.
- [67] A. Al-Fhaid, S. Serra-Capizzano, D. Sesana, M. Zaka Ullah, Singular-value (and eigenvalue) distribution and Krylov preconditioning of sequences of sampling matrices approximating integral operators, *Numer. Linear Algebra Appl.* 21 (6) (2014) 722–743.